



FRACTURE ZONE DETECTION USING VERY LOW FREQUENCY ELECTROMAGNETIC METHOD (VLF-EM) OF GEOPHYSICAL PROSPECTING FOR GROUNDWATER IN ORU-IJEBU SOUTH-WEST NIGERIA

Ishola S. A.

*Department of Earth Sciences, Olabisi Onabanjo University Ago-Iwoye, P.M.B 2002, Ago-Iwoye,
Ogun State Nigeria*

Corresponding author's email: ishola.sakirudeen@oouagoiwoye.edu.ng

Keywords: Very Low Frequency, Fracture Zone, Oru, Geonics EM-16GL, Hydrologic

ABSTRACT: Very low frequency (VLF) electromagnetic method was conducted to study fracture zone detection as part geophysical assessment and preliminary exploration for groundwater studies were carried out in Oru-Ijebu; locations which lies within the Crystalline Basement Complex rock of Southwestern Nigeria with the aim of delineating subsurface structures associated with groundwater occurrence by determining the depth and lateral extent of conductive zones inferred as major aquifers in the study area. A total of twelve (12) profiles were covered during VLF field data acquisition with 10m sample interval along each profile with spread length ranging between 100m and 200m using Geonics EM-16GL instrument. The acquired VLF data were processed and interpreted using Karous-Hjelt software to generate the 2-D conductivity image of the subsurface with emphasis placed on the Fraser filtered plot which transformed genuine cross-over points in peaks and pseudosection. The results of the study showed the presence of fracture zones and are prominently oriented in the NE-SW and NW-SE direction. The result also revealed that most of the fractured zones were located at a depth range of 0 to 30m within the subsurface. The presence and interconnectivity of the fractured zones show that the study area has good prospects for groundwater. The study therefore recommends the drilling for prospective and suitable boreholes at locations VLF-ORU01, VLF-ORU02, VLF-ORU04, VLF-ORU05, VLF-ORU07 and VLF-ORU012 between 50-75m, 120-165m, 30-50m, 165-200m, 170-190m, and 83-100m respectively along the profile. The most conductive zone was found at VLF-ORU03 at a lateral extent of 70-105m, while the least conductive zone was identified at VLF-ORU01 at a lateral extent of 125-165m. Therefore, on the basis of the investigation, the drilling of productive boreholes suitable for groundwater exploration are recommended at the traverses identified above.

Ishola S. A



INTRODUCTION

Groundwater is a vital component of Earth's hydrological cycle, refers to water that resides beneath the Earth's surface within the saturated zones of soil and rock formations. It plays a crucial role in sustaining ecosystems providing drinking water for communities, supporting agriculture, and fueling industrial processes (Shekhar, 2017). Groundwater originates from atmospheric precipitation through direct rainfall, infiltrates into the ground, rivers, canals, lakes, and accumulates in underground reservoirs, and is stored within geological formations (Ariyo and Osinowo, 2007; Okafor and Mamah, 2012). The occurrence and movement of groundwater in an area are governed by several factors such as topography, lithology, geological structures, depth of weathering extent of fracture, secondary porosity, soil, drainage pattern, landforms, land use/land cover, climatic conditions and interrelationship between these factors. The rapid population growth has increased the demand for groundwater. Excess availability of potable water in communities provides the foundation for their prosperity because a water crisis would have undesirable effects on agricultural practices, economic activities, and domestic life (Selvam *et al.*, 2015; Awosika *et al.*, 2020; Mushtaq *et al.*, 2019; Sharma *et al.*, 2021; Oketayo *et al.*, 2022a).

The mapping of fracture zone which is a break in crystalline basement rock due to tectonic forces or intrusion of magmatic bodies is

important for civil engineering and hydrogeological applications. In civil engineering, it helps to locate the safest depth to lay the foundation of buildings. The geological significance of fracture zones in hydrogeology is that it determines the competency of the underlie rocks. Areas that are extensively fractured and where the fractures are deep are considered as weak zones and considered suitable zones for groundwater development (Alagbe *et al.*, 2013) But areas that are slightly fractured and where fractures are not deep are considered as competent zones and are considered better sites for engineering purposes (Sunmonu *et al.*, 2011). The drilling of test wells for fluid studies and the determination of hydraulic properties of subsurface rocks is an expensive method. Surface geophysical methods had been proven to be a rapid, inexpensive complement to drilling for determining the locations and orientation of fracture zone in bedrock (George *et al.*, 2013). They can be used in conjunction with geologic, hydrogeologic and borehole techniques to optimize well sitting (Jansein and Juncsek, 1997) or as a 'stand alone' method of fracture detection (George *et al.*, 2013), (Lieblich *et al.*, 1991), (Haeni *et al.*, 1993) and assessment of leach ate plume migration in disposal sites (Jegade *et al.*, 2011). In hard rock areas, groundwater is found in the cracks and fractures of the local rock. Groundwater yield depends on the size of fractures and their interconnectivity. VLF EM method has been applied successfully to map the resistivity



contrast at boundaries of fractured zones having a high degree of connectivity (George *et al.*, 2013). Also, VLF method yields a higher depth of penetration in hard rock areas because of their high resistivity (McNeil and Labson, 1991). VLF method is capable of delineating fractures in lateral direction effectively compared to resistivity sounding (Sharma and Baranwal, 2005), characterize aquifer structures in a complex environment (Ozegin *et al.*, 2012), underground water contamination by solid waste (Deborah and Ayobami, 2013), examine the fault pattern of industrial estate (Theophilus and Lukman, 2012). This study was driven by the desire to investigate water bearing fracture zones in Oru-Ijebu using very low frequency (VLF) electromagnetic method. Oru is a community whose population is continuously on the increase by the daily influx of biological population mostly students due to its proximity to Olabisi Onabanjo main and mini campuses. The inhabitants of Oru community are battling with the problems of inadequate availability of potable water for their daily activities due to the progressive population growth that has led to severe shortage of potable water for the area which in turn poses a great challenge to both the indigenes, students and the government staffs. To meet the needs of this aforementioned growing population, it is quite necessary to source for further and alternative water supply sources. The households and residents of Oru-Ijebu community are mostly depending on shallow hand-dug wells most of which are

uncovered for household activities. These water sources are susceptible to pollutions due to their exposure to environmental activities like dust, surface run-off from nearby dumpsites and so on. The continued use of water directly from these sources may lead to water borne diseases like cyclosporiasis, amoebiasis, hepatitis A, cholera, diarrhoea, bilharzias among others. Furthermore, women, children, students, spend a lot of time and effort everyday going to the nearby wells sites to fetch water. These practices affect the productivity of these women, children, students and entire community at large. Sometimes students waste precious school hours outside classrooms in search of water at the expense of their academic engagement. The study area is a basement complex in Southwestern Nigeria whose groundwater potential mapping is relatively complex due largely to the highly variable nature of the geological terrain (Anbazhagan *et al.*, 2011) extensive hydrogeological investigations are required in basement complex environment to understand groundwater conditions (Bayewu *et al.*, 2017).

The location and orientation of fracture zones are important for the exploration of groundwater, modeling fluid flow, and contaminant transport in fractured rocks. Surface geophysical methods are rapid and inexpensive aids to the drilling for determining the locations and orientation of fractured zones in bedrocks (Jamal and Singh, 2018). Surface geophysical methods in conjunction with



geologic, hydrologic, and borehole-geophysical investigations can be used to optimize well location, or as a stand-alone method of fracture detection (Jamal and Singh, 2018). Groundwater occurrence in the hard rock terrain can be very irregular due to abrupt discontinuity in lithology, thickness, and electrical properties of the overburdened and weathered bedrock (UdayaLaxmi and Ramadass, 2013; Selvani *et al.*, 2015). Exploration of groundwater in hard rock terrain is a challenging task when promising groundwater zones are associated with fractured and fissured media. In this environment, the groundwater potentiality depends mainly on the thickness of the weathered/fractured layer overlying the basement (Mansour, 2018) and the water yield depends on the size of the fractures and their interconnectivity. VLF EM method has been applied successfully to map the resistivity contrast at boundaries of fractured zones having a high degree of connectivity and yields a higher depth of penetration in hard rock areas because of their high resistivity (Jamal and Singh, 2018). VLF method is capable of delineating fractures in lateral direction effectively compared to the resistivity sounding (Sharma and Baranwal, 2005), and in characterizing aquifer structures in a complex environment (Ozegin *et al.*, 2012). The VLF-EM method is widely used for the detection of buried conductive targets, including aquiferous faulting systems (Jamal and Singh, 2018). It offers relatively a fast approach to

delineating the fractures. The advantage of this technique is that the measurements are easy to interpret in a qualitative manner (Vargemezis, 2007). The VLF-EM investigation involved mapping the terrain in terms of the conductivity distribution, which can provide salient information about some structural features such as fractures, joints, or faults as well as delineate the thickness of the weathered profile based on a conductivity contrast between the saturated weathered layer and the unfractured crystalline basement rocks (Osinowo and Olayinka, 2012).

2.0 Study Area

2.1 Location and Accessibility

The study area is located in Oru, Ijebu, Southwestern Nigeria. It falls between latitudes $6^{\circ} 56'$ to $6^{\circ} 58'$ North of the Equator and longitudes $3^{\circ} 56'$ to $3^{\circ} 58'$ East of the Greenwich Meridian. Oru –Ijebu lies at a distance of about 461 km from the equator within the equatorial belt of Nigeria at longitude $3^{\circ} 55'$ to $3^{\circ} 58'$ east of the Greenwich Meridian and at latitude $6^{\circ} 56'$ to $6^{\circ} 58'$ North of the equator. The study area is surrounded by the neighboring towns of Ilaporu, Awa, Ijebu-Igbo, and Ago-Iwoye. The study area is accessible through major roads and footpaths. The town is located within Ijebu –North Local Government Area of Ogun State (Fig. 1). Oru, is a semi urban town in Ijebu North Local Government Area of Ogun State, Nigeria, covering an area of 300 km². Geologically, Oru is made up of two main rock types: the basement complex rock of the Precambrian which is made up of the older and



younger granites and the sedimentary layers rocks which consist of cretaceous, tertiary and quaternary sediments. The drainage shows a dendritic drainage pattern and the major river in the area is River Ereru which flows southerly through the study area and all other tributaries take their source from this river. The study is located within the equatorial rain forest and guinea savanna vegetation having tall grasses, shrubs and scattered trees which are well grown (Adeoti *et al.*, 2016). Its topography is characterized by a wide area of undulating lowland, sandy type of soil combining small amount of clay. Average temperature ranges between 29° to 30°C (Adesanya, 2018), with tropical climatic condition having 2 major seasons; the dry and rainy season. The average rainfall is between 28mm to 40mm, peaking between May and August annually. The vegetation is within the equatorial rain forest and guinea savanna vegetation having tall grasses, shrubs, and scattered trees that are well-grown. Its topography is characterized by a wide area of undulating lowland, sandy type of soil combining small amounts of clay (Oketayo *et al.*, 2022b). Socio-demographically agriculture is the main occupation of Oru people; farmers cultivate variety of crops such as yam, cassava, maize, rice, plantain, beans, vegetables and citrus fruits such as orange, paw-paw, pineapple and so on. Although the main cash crops produced in the area are cocoa, cashews, kola nut, oil palm and palm kernels (Adeoti *et al.*, 2016).

2.2 Geology of the Study Area

The study area, Oru, and its environs lie within the Basement Complex of southwestern Nigeria. It forms part of the Pan African mobile belt which lies to the east of West African Craton. The major rock types in the area of study include granite gneiss, granite, banded gneiss, pegmatite, and undifferentiated migmatite and these have been intruded by quartz veins and pegmatite veins. Granite gneiss is the major rock that dominated the study area. They are typically medium-grained in texture and the minerals present include quartz, biotite, plagioclase, orthoclase, and other accessory minerals. There is a considerable variation in the amount of mafic and felsic minerals. Granite gneiss stretches from the eastern part to the northwest of the area (Ishola *et al.*, 2023). Generally, it is grey and texturally medium-grained. Mineralogically, it consists of quartz, plagioclase, feldspar, biotite, and hornblende. Granite is the second most abundant rock type in the area covering the entire eastern and northwestern region. The colour is grey and texturally medium-grained. Banded Gneisses are foliated and the rocks consist of alternating bands of light and dark minerals. The light band is composed of felsic minerals mainly quartz and feldspar while the dark band consists of mafic minerals. Mineralogically, banded gneiss contains both felsic and mafic minerals. Pegmatite is located in the western part of the area of study. The entire Oru Township is underlain by pink pegmatite. Pegmatite is a very coarse-grained minor igneous rock; they are formed from the residual magma that is rich in volatile and fugitive elements. They occur as massive intrusions in Oru. Texturally, it ranges from medium to coarse-grained.

Ishola S. A



Mineralogically, feldspar, mica (muscovite dominating over biotite), and quartz are the most abundant minerals while muscovite and tourmaline occur as accessory minerals (Ishola

and Olufemi, 2024). Figure 1 below shows the Geological Map of the study area while figure represent the location and accessibility map of the study area.

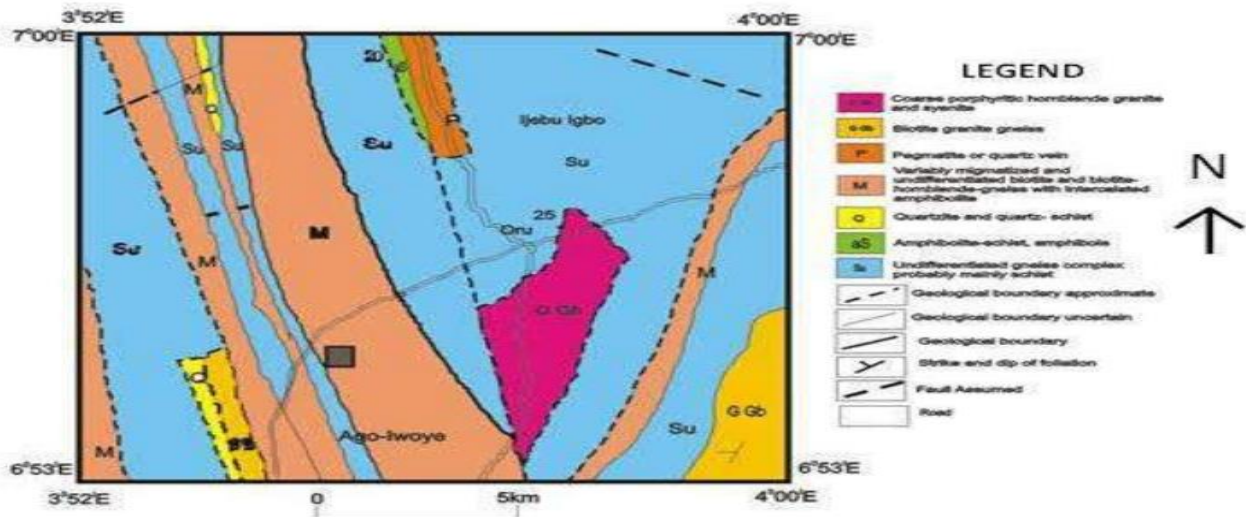


Figure 1: Geological Map of the Study Area. (Adekoya *et al.*, 2017)

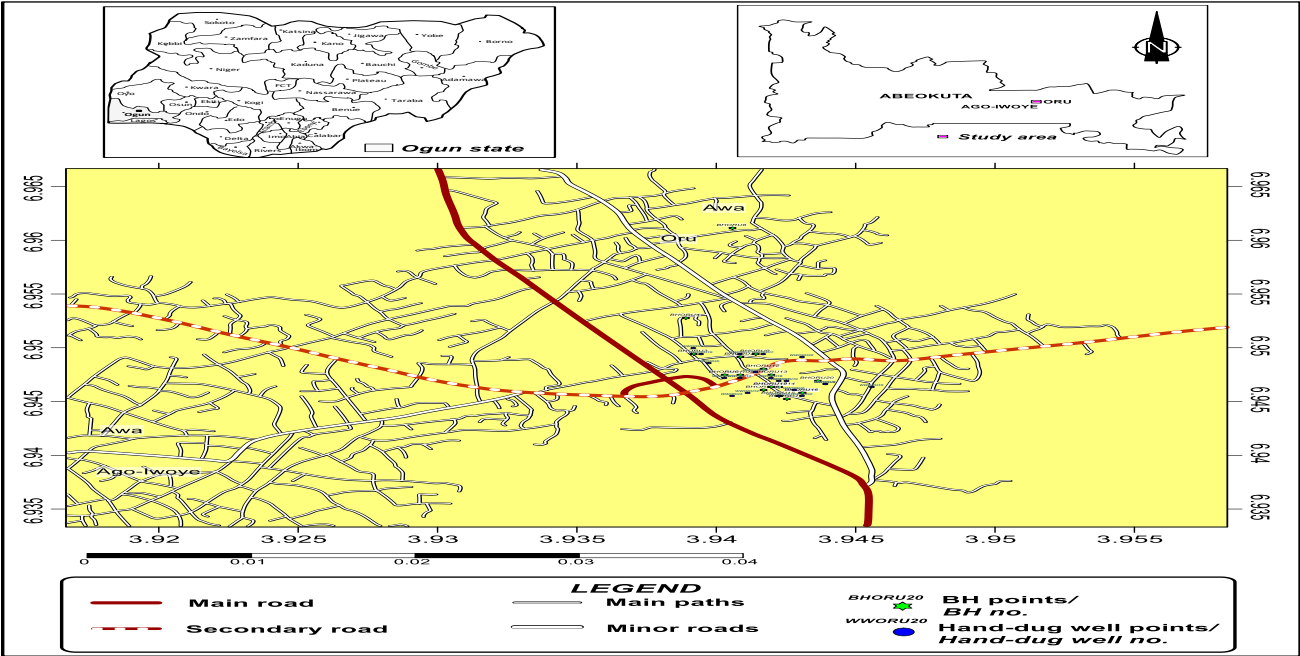


Figure 2: Location and accessibility map of the study area (Ishola, 2024)

Ishola S. A



3.0 Materials and Methods

3.1 Theoretical Background

Basic Principle of Electromagnetic Method

The basic principle of electromagnetic (EM) methods in geophysics relies on the interaction between time-varying electromagnetic fields and subsurface materials, which is fundamentally described by Maxwell's equations. These equations govern how electric fields and magnetic fields are generated and how they propagate through space and interact with materials. When an alternating current flows through a transmitter coil on the surface, it generates a primary electromagnetic field that penetrates the ground. As this primary field interacts with conductive materials in the subsurface, it induces eddy currents within these materials due to electromagnetic induction (Telford *et al.*, 1990). According to Faraday's Law, a changing magnetic field generates an electric field, and this electric field drives the eddy currents, which, in turn, generate their own secondary magnetic fields. The strength and decay of these secondary fields depend on the electrical conductivity and permeability of the subsurface materials, as well as the frequency of the primary field (McNeil, 1980; Ward, 1988). The depth of penetration, or skin depth, of the electromagnetic fields, is inversely related to the square root of the product of the material's conductivity, magnetic permeability, and the frequency of the applied field, meaning that higher frequencies or more

conductive materials result in shallower penetration (Ward and Hohmann, 1988; Telford *et al.*, 1990; Reynolds, 1997). By measuring the secondary fields at the surface with receiver coils, geophysicists can analyze the data to infer the conductivity distribution and identify subsurface structures. This technique is widely applied in various fields such as mineral exploration, hydrocarbon detection, groundwater studies, and environmental monitoring, due to its non-invasive nature and ability to provide detailed subsurface information.

Maxwell's equations are a set of four fundamental equations that form the foundation of classical electromagnetism, classical optics, and electric circuits. They describe how electric and magnetic fields are generated and altered by each other and by charges and currents. The equations are crucial for understanding a wide range of physical phenomena and are instrumental in the development of many modern technologies (Telford *et al.*, 1990; Reynolds, 1997).

Gauss's Law, the first of Maxwell's equations, is a statement about the relationship between electric charges and electric fields. Mathematically, it is expressed as in equation 1.1 and 1.2.

$$\nabla \cdot D = \rho$$

.....
1.1
or in integral form:



$$\oint_S D \cdot \partial A = \int_V \rho \cdot \partial v \quad \dots\dots\dots 1.2$$

Here, ‘*D*’ is the electric displacement field, ρ is the charge density, ‘*S*’ is a closed surface, and ‘*V*’ is the volume enclosed by ‘*S*’. This equation states that the electric flux through any closed surface is proportional to the total charge enclosed within that surface. Physically, it means that electric charges are sources of the electric field: positive charges create outward field lines, while negative charges create inward field lines. Gauss's Law is fundamental in electrostatics, providing a method to calculate electric fields around charged objects by using symmetry arguments.

Gauss's Law for Magnetism asserts that there are no magnetic monopoles, meaning that magnetic field lines neither begin nor end but always form closed loops. This is represented in equation 2.1 and 2.2 as the first of Maxwell's equations

$$\nabla \cdot B = 0 \quad \dots\dots\dots 2.1$$

and in integral form:

$$\oint_S B \cdot dA = 0 \quad \dots\dots\dots 2.2$$

In these equations, ‘*B*’ is the magnetic flux density. The absence of magnetic monopoles implies that the net magnetic flux through any closed surface is zero. This law is pivotal in magnetostatics and has profound implications for the symmetry of magnetic fields. It also underpins the concept that magnetic field lines

are continuous loops, which is a cornerstone in the understanding of magnetic field topology.

Faraday's Law of Induction is the third Maxwell equation and describes how a time-varying magnetic field induces an electric field. It is expressed below in equation 3.1 and 3.2.

$$\nabla \times E = -\frac{\partial B}{\partial t} \quad \dots\dots\dots 3.1$$

and in integral form:

$$\oint_C E \cdot dl = -\frac{d}{dt} \int_S B \cdot dA \quad \dots\dots\dots 3.2$$

Here, ‘*E*’ is the electric field, ‘*C*’ is a closed loop, and ‘*S*’ is the surface bounded by ‘*C*’. Faraday's Law states that the electromotive force (EMF) around a closed loop is equal to the negative rate of change of the magnetic flux through the surface bounded by the loop. This principle is the foundation of many electrical technologies, including transformers, inductors, and generators. It encapsulates the concept of electromagnetic induction, where a changing magnetic field generates a circulating electric field.

The fourth and final Maxwell equation, **Ampère's Law**, relates magnetic fields to the electric currents and changing electric fields that produce them. It was initially formulated by André-Marie Ampère and later modified by Maxwell to include the displacement current term. The differential form is displayed in equation 4.1 and 4.2

$$\nabla \times H = J + \frac{\partial D}{\partial t} \quad \dots\dots\dots 4.1$$



and the integral form is:

$$\oint_C \mathbf{H} \cdot d\mathbf{l} = \int_S \mathbf{J} \cdot d\mathbf{A} + \int_S \frac{\partial \mathbf{D}}{\partial t} \cdot d\mathbf{A} \dots\dots\dots 4.2$$

In these equations, ‘H’ is the magnetic field strength; ‘J’ is the current density, and $\frac{\partial \mathbf{D}}{\partial t}$ is the displacement current density. This law indicates that magnetic fields are generated both by electric currents and by time-varying electric fields. Maxwell's addition of the displacement current term was crucial for the consistency of the equations and for predicting the existence of electromagnetic waves, which can propagate through empty space.

Electromagnetic (EM) waves are pivotal in geophysical exploration, offering insights into the Earth's subsurface through non-invasive techniques (Ward and Hohmann, 1988). In geophysics, EM fields can be generated by passing an alternating current through a core made up of many turns of wire or through a large loop of wire. These fields are employed to probe subsurface structures, mineral deposits, groundwater, and other geological features. An electromagnetic field is created when an alternating current (AC) flows through a conductor. In geophysical applications, this conductor is often a coil of wire or a large loop.

Bypassing an AC through these configurations, a time-varying magnetic field is produced, which, in turn, induces an electric field according to Faraday's Law of Induction (Telford *et al.*, 1990). For geophysical purposes, the frequencies of the primary alternating field are typically less than a few thousand Hertz. This low frequency range ensures deep penetration into the Earth's subsurface, allowing for the investigation of geological features at significant depths. The wavelength of the primary EM wave used in geophysical surveys ranges from 10 to 100 kilometers. Despite the large wavelength, the separation between the source (transmitter) and the receiver is much smaller. This setup allows for efficient measurement of the secondary fields generated by the interaction of the primary EM field with subsurface materials (Hecht, 2002). Due to the large wavelength relative to the source-receiver distance, the propagation of the primary wave (Figure 3.3) and its associated attenuation can often be disregarded. This simplification is beneficial in interpreting geophysical data, as it focuses on the secondary responses from subsurface features rather than the primary wave itself.

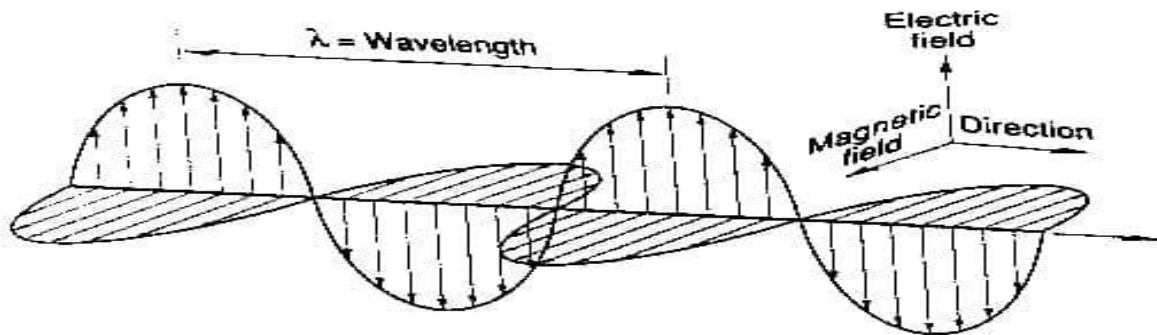


Figure 3.3: The direction of propagation of the electromagnetic wave (Smith and Kearey, 2003).



Frequency-Domain Electromagnetics (FDEM) is another active EM surveying technique that uses continuous sinusoidal currents at various frequencies to generate primary EM fields. The response of the subsurface to these fields is measured to determine conductivity variations. Additionally, an inversion program can be used to interpret the data and obtain the map distribution of electrical conductivity with depth (Auken and Christiansen, 2004). FDEM systems consist of a transmitter, which generates the primary field, and a receiver, which detects the secondary fields. FDEM is used in mineral exploration, environmental assessments, and archaeological surveys. It is effective for shallow subsurface investigations.

The primary field is the initial electromagnetic field generated by the source. This source can be natural, such as the Earth's magnetic field, or artificial, such as an EM transmitter used in surveys. The primary field propagates through the air and into the ground, interacting with the subsurface materials (Reynolds, 2011). The primary field is produced by passing an alternating current through a coil or loop of wire, creating a time-varying magnetic field. This can be done using different frequencies depending on the survey requirements. As the primary field propagates through the subsurface, it induces currents in conductive materials according to Faraday's Law of Induction. The primary field itself is relatively straightforward to model and predict because it does not yet carry information about

subsurface structures (Telford *et al.*, 1990). The primary field is essential because it sets up the conditions for inducing secondary fields in the subsurface. Its characteristics, such as frequency and strength, influence the depth of penetration and the resolution of the survey (Nabighian, 1988).

The secondary field is the electromagnetic response generated by the subsurface materials in reaction to the primary field. When the primary field interacts with conductive or magnetic materials underground, it induces currents, which in turn create their own electromagnetic fields. These induced fields are called secondary fields (Ward, 1990). Secondary fields are generated through the process of electromagnetic induction, where the primary field induces eddy currents in conductive materials. These eddy currents produce their magnetic fields, which are detected by receivers on the surface (Kaufman and Keller, 1983). The secondary fields are detected using various sensors and instruments. The characteristics of these fields such as their amplitude, phase, and decay rate, provide valuable information about the electrical properties and distribution of subsurface materials (Chave and Jones, 2012). The secondary fields carry information about the subsurface conductivity and structure. By analyzing the secondary fields, geophysicists can infer the presence of different materials, such as ores, groundwater, or contaminants, and can map subsurface features (Everett, 2013).



The interaction and interpretation between primary and secondary fields can be complex. The amplitude and phase of the secondary field relative to the primary field provide clues about the conductivity and permittivity of the subsurface materials. High-conductivity materials will cause stronger secondary fields with significant phase shifts (Milsom and Eriksen, 2011). As EM waves travel through different materials, they are attenuated and distorted. Highly conductive materials will attenuate the EM waves more, reducing the strength of both primary and secondary fields as depth increases. This attenuation must be accounted for in data interpretation. Advanced computational techniques, such as forward modeling and inversion, are used to simulate the primary and secondary fields and to match observed data with theoretical models. This process helps to create detailed subsurface images and maps, revealing the geological structures and materials present (Smith and Kearey, 2003).

The depth of penetration of an electromagnetic (EM) field into a material is a crucial parameter in geophysical surveys, as it determines how deep the EM waves can effectively probe into the Earth's subsurface. This depth is influenced primarily by the frequency of the EM waves and the electrical conductivity of the medium.

The amplitude of EM fields decreases exponentially with depth. This means that as the EM wave travels deeper into the subsurface; its amplitude diminishes at an exponential rate.

The relationship between the amplitude of the EM radiation at depth A_d and its original surface amplitude A_0 is given by the formula:

$$A_d = A_0 e^{-z/d} \dots\dots\dots 5$$

where z is the depth, and d is the penetration depth, which is the depth at which the amplitude is decreased by a factor of e^{-1} (approximately 0.37) compared to its surface amplitude.

The penetration depth d can be defined as the depth at which the amplitude A_d is decreased by the factor e^{-1} compared to its surface amplitude. The penetration depth d is given by:

$$d = \frac{503\sqrt{\rho}}{f} \dots\dots\dots 6$$

where:

- d is the penetration depth in meters.
- ρ is the resistivity of the medium in ohm-meters (Ωm).
- f is the frequency of the EM wave in Hertz (Hz).

Equation 5 and 6 show that the penetration depth increases with increasing resistivity and decreases with increasing frequency.

In practical geophysical surveys, the choice of frequency and an understanding of the subsurface conductivity are critical for optimizing the depth of investigation. For example, Lower Frequencies used in surveys aimed at probing deeper geological structures, such as in mineral exploration or groundwater studies while the Higher Frequencies are suitable for shallow investigations, such as in environmental studies or archaeological



surveys, where detailed near-surface resolution is required. By carefully selecting the appropriate frequency and considering the conductivity of the subsurface materials, geophysicists can tailor their surveys to effectively investigate the desired depth, revealing valuable information about the subsurface composition and structure.

Very Low Frequency Electromagnetic (VLF-EM) Method

The source utilized by the VLF-EM is electromagnetic radiation generated in the low-frequency band ranging from 15.0–25.0 kHz by the powerful radio transmitters utilized in long-range communications and navigational systems. There are several available stations across the globe that utilize this frequency range for continuous transmission either functioning as an unmodulated carrier wave superimposed morse code; such signals may be employed for surveying up to distances of several thousand kilometers from the transmitter. The electromagnetic field is essentially planar and horizontal at large distances from the source (Telford *et al.*, 1990; Reynolds, 1997; Parasnis, 1996; Pedley *et al.*, 2000). The electrical component E lies in a vertical lane and the magnetic component H lies at right angles to the direction of propagation in a horizontal plane. A conductor that strikes in the direction of the transmitter is cut by the magnetic vector and the induced eddy currents produce a secondary electromagnetic field. Conductors striking at right angles to the direction of propagation are not cut effectively by the magnetic vectors (Telford *et al.*, 1990; Reynolds, 1997). The basic VLF-EM receiver is a small hand-held device incorporating two orthogonal

aerials which can be tuned to the particular frequencies of the transmitters. The direction of a transmitter is found by rotating the horizontal coil around a vertical axis until a null position is found. Traverses are then performed over the survey area at right angles to this direction (Reynolds, 1997). The instrument is rotated about a horizontal axis orthogonal to the traverse and the tilt recorded at the null position. Modern instruments have three coils with their axes at right angles. They can thus detect the signal whatever its direction and find out the null orientation electronically and automatically. Some instruments will measure signals from two or more transmitters simultaneously. In this case, transmitters are chosen based on whose signals arrive in the survey area at very different azimuths (Parasnis, 1996; Pedley *et al.*, 2000; Smith and Kearey, 2003). The VLF-EM has the advantages that the field equipment is small and light, being conveniently operated by one person, and there is no need to install a transmitter. However, for a particular survey area, there may be no suitable transmitter providing a magnetic vector across the geological strike. A further disadvantage is that the depth of penetration is somewhat less than that attainable by tilt-angle methods using a local transmitter.

3.2 Field Data Acquisition

The survey was carried out using Geonics EM-16GL instrument with a frequency of 16 kHz along with other accessories such as hand-held Global Positioning System (GPS), and measuring tape was used for the acquisition of the EM data (Figure 3.4). The VLF data was acquired only after locating the transmitter direction. After the transmitter direction was

established, the receiver was moved vertically (up, and down) perpendicular to the transmitter direction to enable the acquisition of good-quality data with minimum noise

The geophysical data was collected along a total of twelve (12) traverses, with profile lengths from each profile stations ranging from 100 m to 200 m (Figures 3.1 and 3.2). Readings were taken at an inter-spacing of 5m and 10 m in the twelve locations with profile lines oriented in N-S, E-W directions respectively. Also, the direction of the transmitting stations was perpendicular or nearly perpendicular to the

traverse before readings were taken. During survey, effort was made to avoid putting traverses in area that contain cultural features that may mask anomalies associated with the intended target strike. Also, the direction of the transmitting station was perpendicular or nearly perpendicular to the traverse before readings were taken. The VLF data was first acquired and interpreted to identify zone (s) or regions with high conductivity that are suggestive of fractured and/or thick weathered layers. The profiles were denoted as VLF-ORU1 to VLF-ORU12.

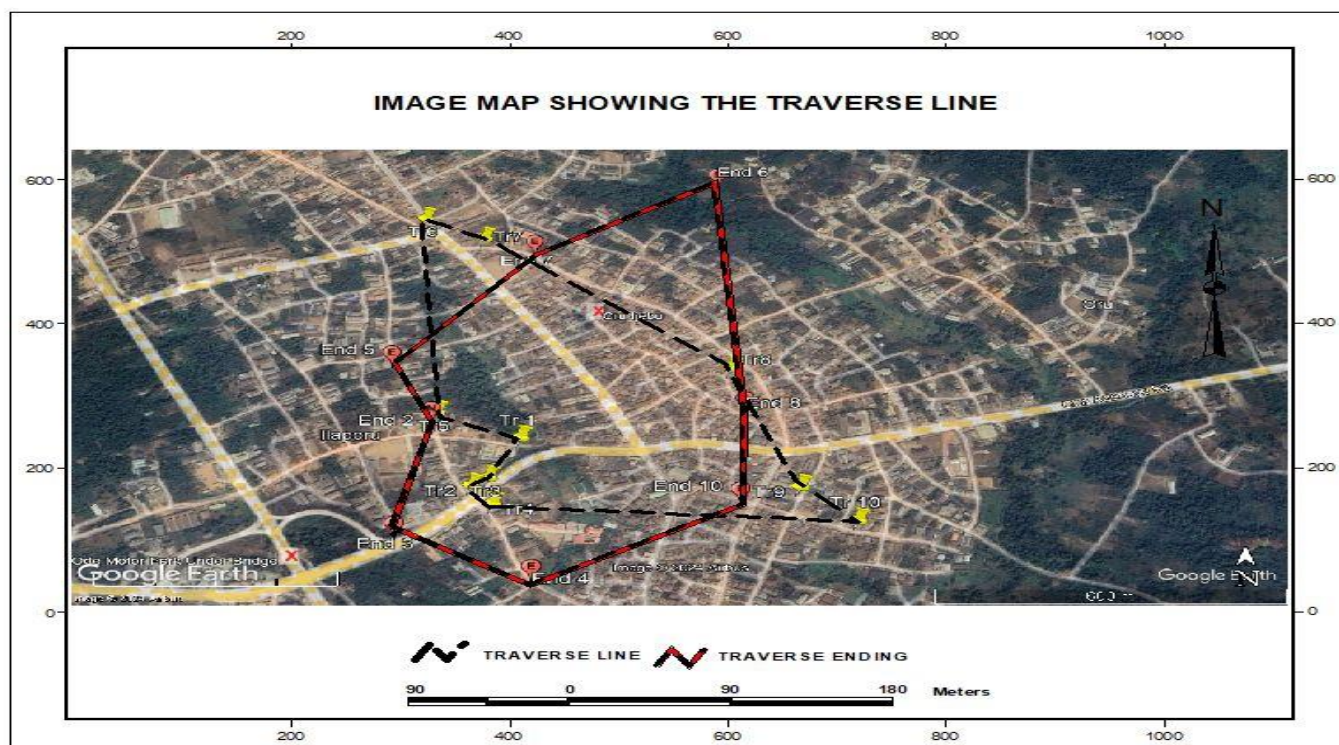


Figure 3.1: Data Acquisition Map showing the Investigated Locations in Google Earth Imagery.

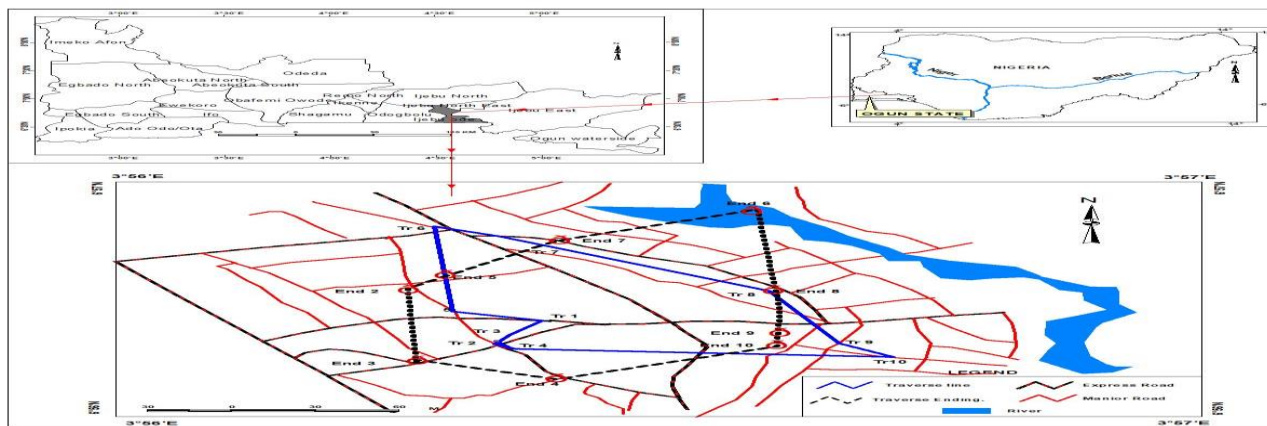


Figure 3.2: Data Acquisition Map showing the study area as an inset map within the Continental margin of Ogun State and South-West Nigeria

3.2 Data Processing and Interpretation

The real and imaginary VLF data were inputted into an Excel worksheet and saved in a data format. This data was then read with the Karous-Hjelt software to generate the 2-D conductivity image of the subsurface. Emphasis is therefore placed on the Fraser filtered plot which helps to transform genuine cross-over points in peaks and the pseudo-section produced by using Karous-Hjelt software. The inversion of the Fraser filtered curve into the current density section provides more information as regards the dimension and depth extent of the conductive zones. High conductive zones are displayed in yellow to red color, while the low current density is depicted in green to blue color (Figure 4.2.1 to 4.2.12).

4.0 RESULTS AND DISCUSSION

The results of the Very Low Frequency Electromagnetic (VLF-EM) method conducted along the traverses in the study area are hereby presented as samples of the Fraser filter results which depicts the plots of filtered in-phase data against distance at each profile station in Figure 4.1.1 to 4.1.12 while the 2-D conductivity sections as obtained from Current density cross section plot of in-phase data against distance at location are presented in Figure 4.2.1 to 4.2.10. The 2-D conductivity sections are indicative of the surface conductivity with depth.

4.1 2-D Conductivity Section along Traverse VLF-ORU1

The Fraser filtering and 2-D conductivity section obtained along traverse 1 is presented in Figures 4.1.1 and 4.2.1. The 2-D section investigated up to 30 m depth beneath the subsurface. The real and imaginary components vary between -30 to -6 and -28 to $+16$ respectively. However, from the 2-D conductivity section, high conductivity regions/zones were identified at lateral distances of about 25 m to 40 m and 50 m to 75 m respectively. These zones are suggestive of possible zones for groundwater accumulation.

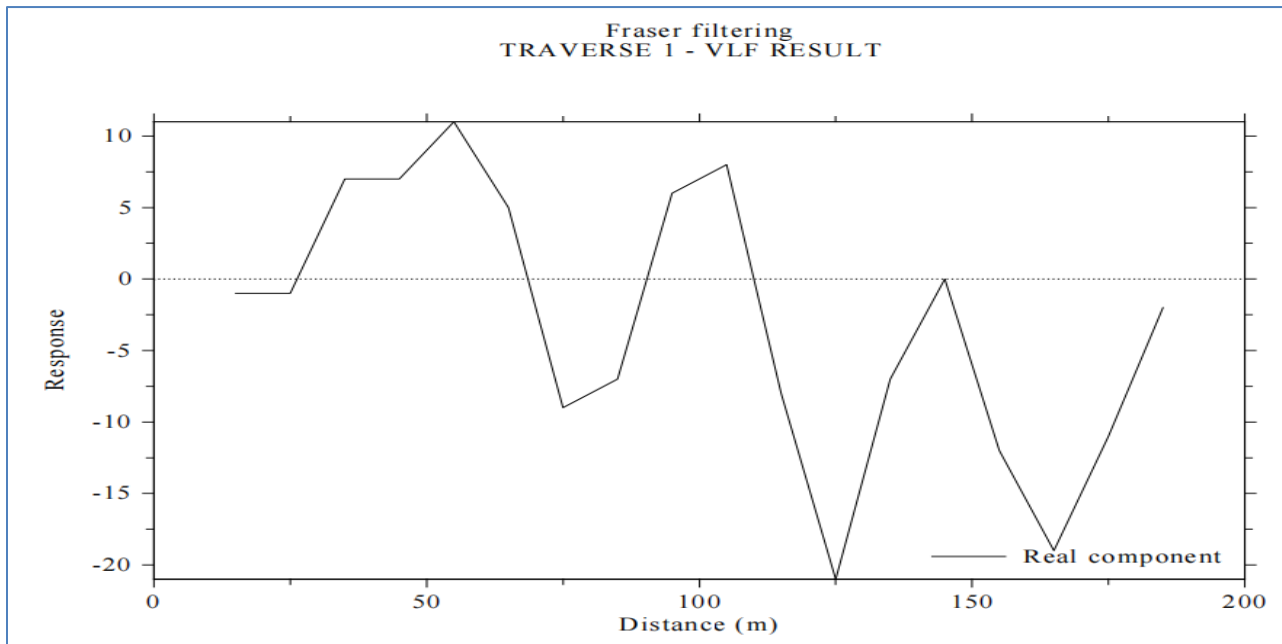


Figure 4.1.1: Fraser Filter Result along Traverse VLF-ORU1

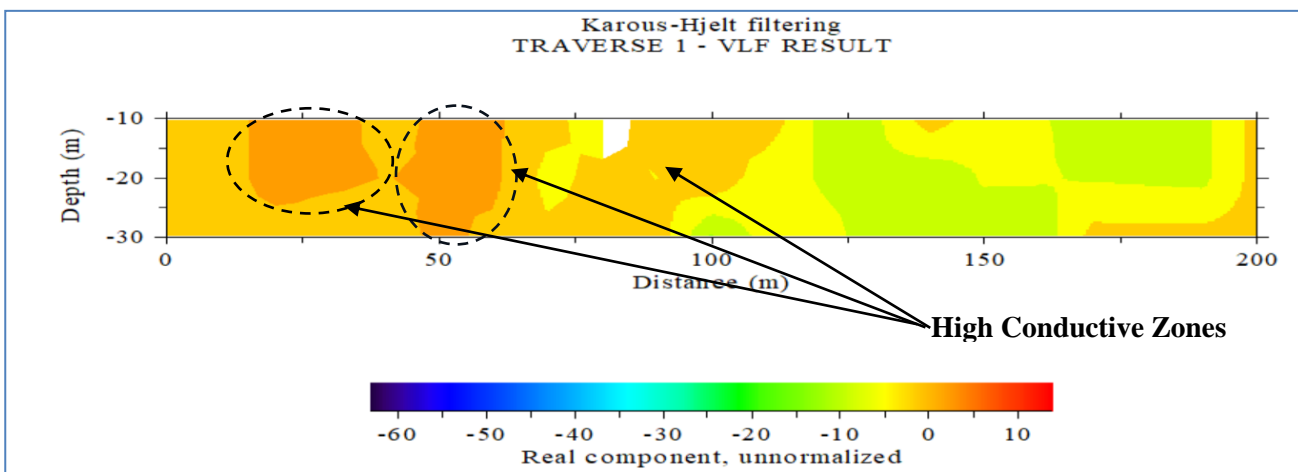


Figure 4.2.1: 2-D Conductivity Section along Traverse VLF-ORU1

4.2. 2-D Conductivity Section along Traverse VLF-ORU2

The Fraser filtering and 2-D conductivity section obtained along traverse 2 is presented in Figures 4.3 and 4.4. The 2-D section investigated up to 30 m depth beneath the subsurface. The real and imaginary components vary between -20 to -5 and -32 to $+22$. However, from the 2-D conductivity section, high conductivity regions/zones were identified at lateral distances of about 20 m to 28 m and 120 m to 165 m respectively. These zones are suggestive of possible zones for groundwater accumulation.

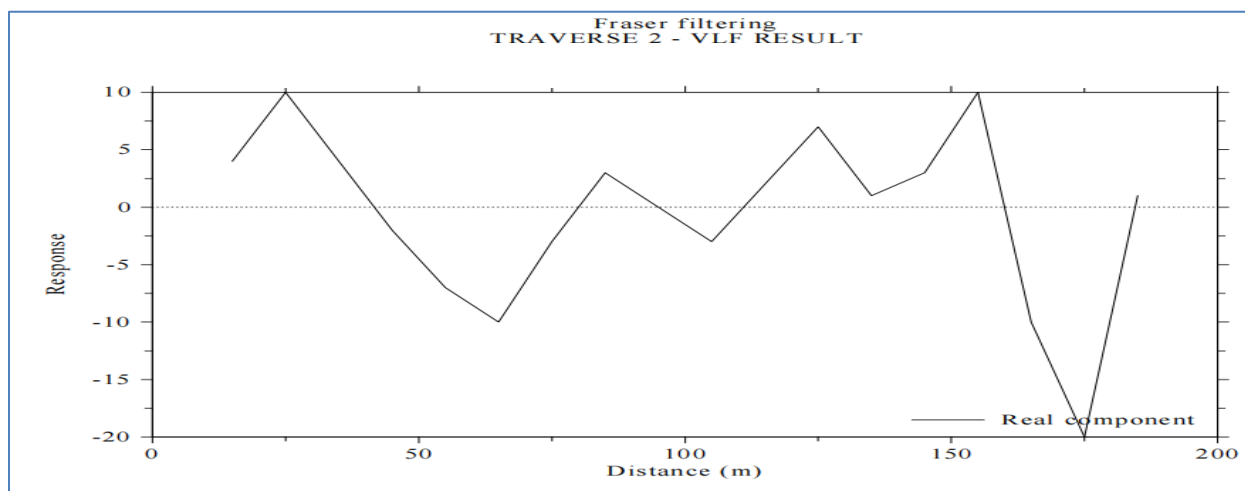


Figure 4.1.2: Fraser Filter Result along Traverse VLF-ORU2

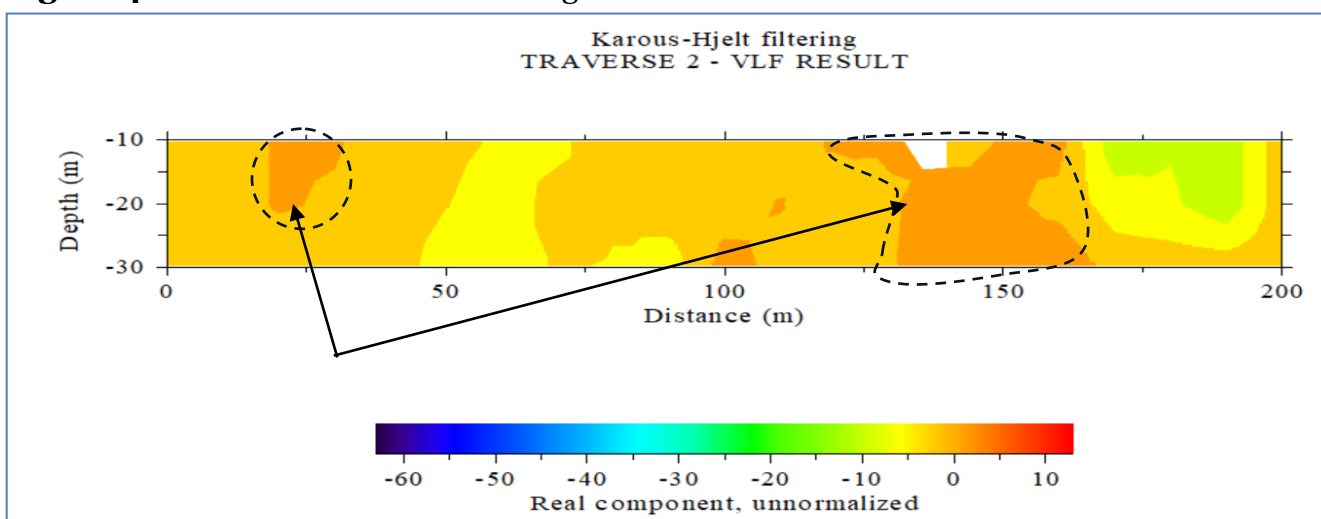


Figure 4.2.2: 2-D Conductivity Section along Traverse VLF-ORU2

4.3 2-D Conductivity Section along Traverse VLF-ORU3

The Fraser filtering and 2-D conductivity section obtained along traverse 3 is presented in Figures 4.1.3 and 4.2.3. The 2-D section investigated up to 30 m depth beneath the subsurface. The real and imaginary components vary between -28 to -5 and -20 to $+20$. However, from the 2-D conductivity section, high conductivity regions/zones were identified at lateral distances of about 17 m to 30 m and 70 m to 105 m respectively. The zone identified at a lateral distance of about 70 m to 105 m represents a possible fractured zone for groundwater accumulation as shown in (Figure 4.6).

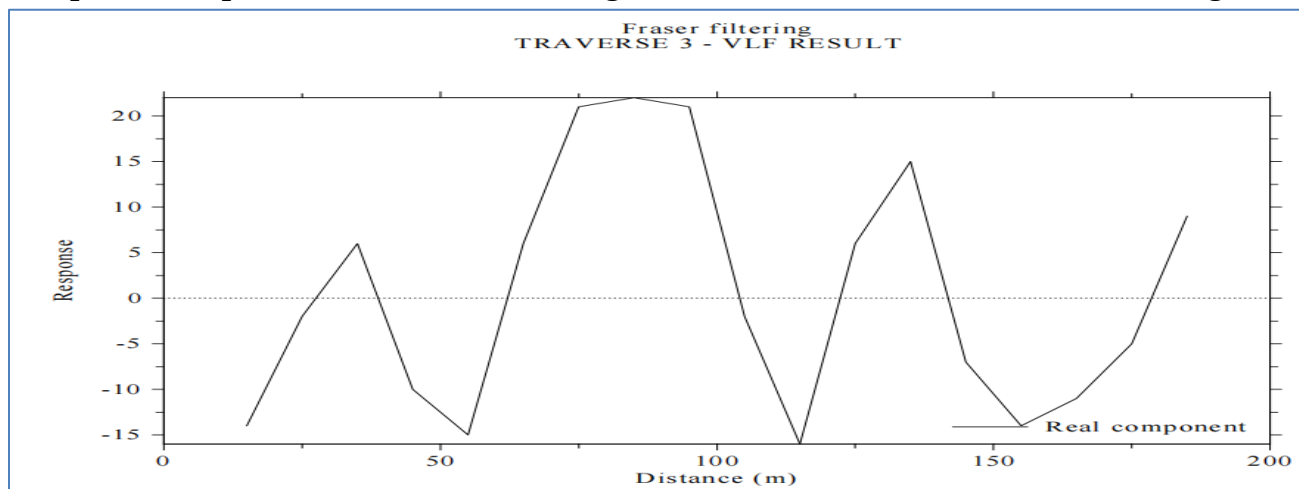
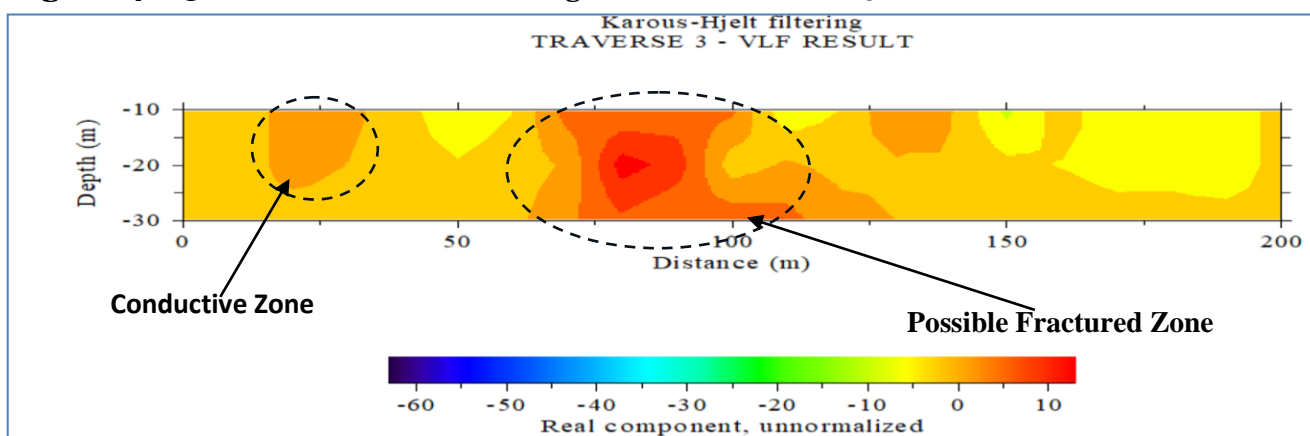


Figure 4.1.3: Fraser Filter Result along Traverse VLF-ORU3



4.4 2-D Conductivity Section along Traverse VLF-ORU4

The Fraser filtering and 2-D conductivity section obtained along traverse 4 is presented in Figure 4.1.4 and 4.2.4. The 2-D section investigated up to 15 m depth beneath the subsurface. The real and imaginary components vary between -30 to -5 and -24 to $+24$. From the 2-D conductivity section, high conductivity regions/zones were identified at lateral distances of about 30 m to 50 m and 82 m to 100 m respectively (Figure 4.8). These zones are suggestive of possible zones for groundwater accumulation.

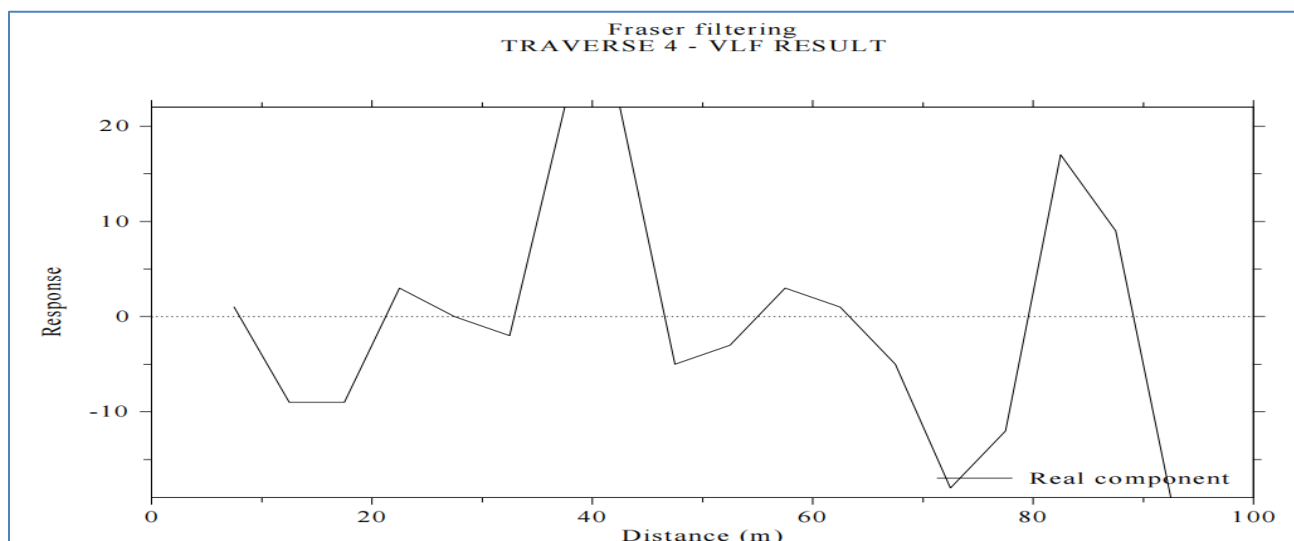
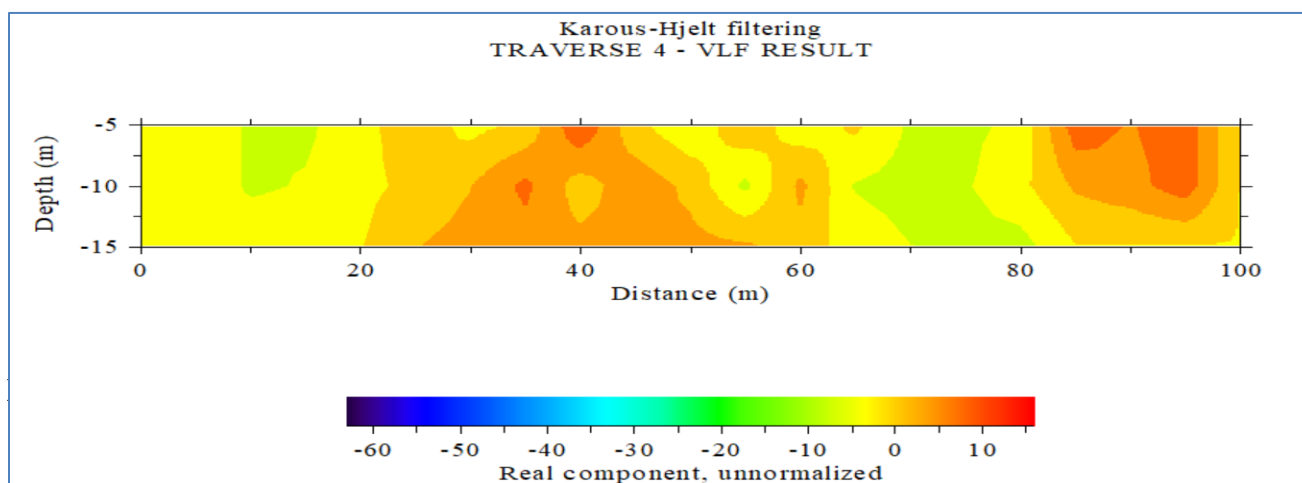


Figure 4.1.4: Fraser Filter Result along Traverse VLF-ORU4



4.5 2-D Conductivity Section along Traverse VLF-ORU5

The Fraser filtering and 2-D conductivity section obtained along traverse 5 is presented in Figures 4.1.5 and 4.2.5. The 2-D section investigated up to 30 m depth beneath the subsurface. The real and imaginary components vary between -22 to -6 and $+5$ to $+26$. From the 2-D conductivity section, three (3) high conductivity/zones were identified at lateral distances of about 12 m to 35 m, 50 m to 90 m, and 165 m to 200 m respectively (Figure 4.1.5). These zones are suggestive of possible zones for groundwater accumulation.

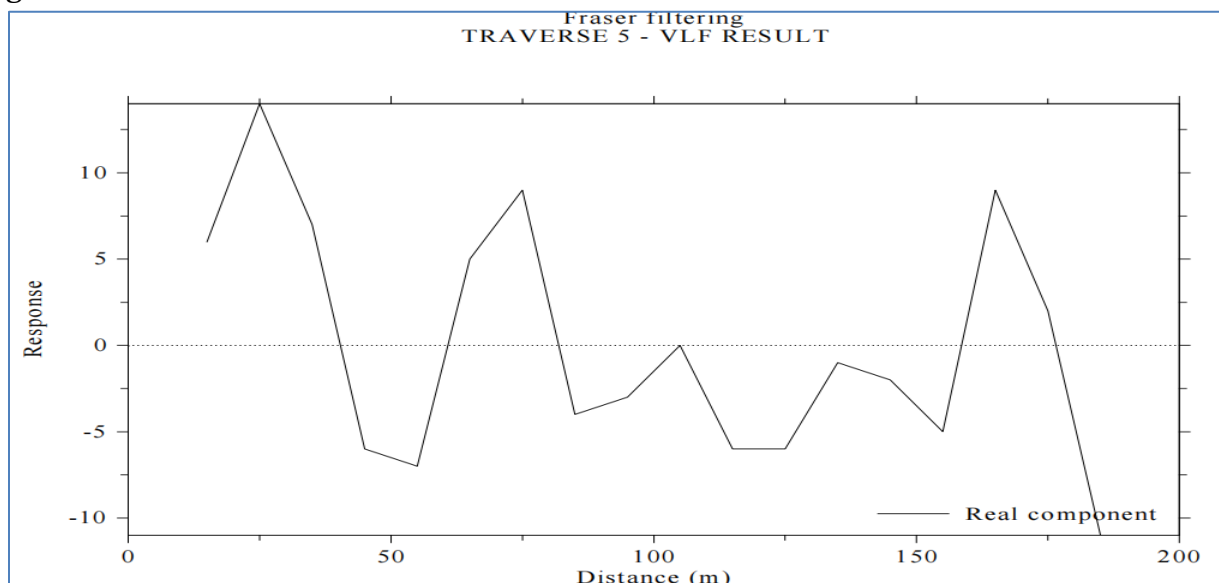


Figure 4.1.5: Fraser Filter Result along Traverse VLF-ORU5

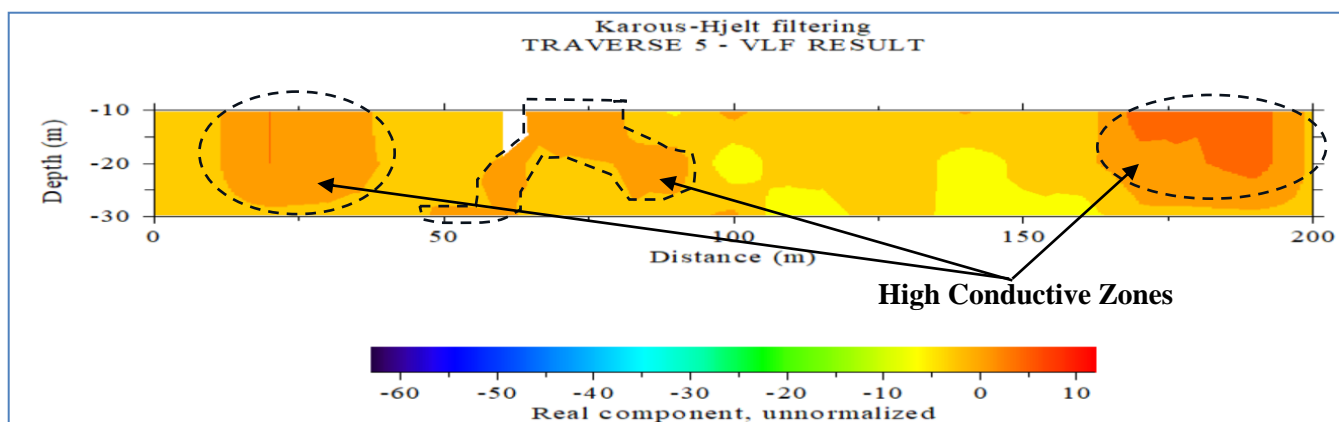


Figure 4.2.5: 2-D Conductivity Section along Traverse VLF-ORU5

4.6 2-D Conductivity Section along Traverse VLF-ORU6

Figures 4.1.6 and 4.2.6 represent the Fraser filtering and 2-D conductivity section results generated for traverse 6. The 2-D section investigated up to 30 m depth beneath the subsurface. The real and imaginary components vary between -25 to -7 and -20 to $+23$. From the 2-D conductivity section, two (2) high conductivity /zones were identified at lateral distances of about 40 m to 55 m and 180 m to 195 m. These zones are suggestive of possible zones for groundwater accumulation.

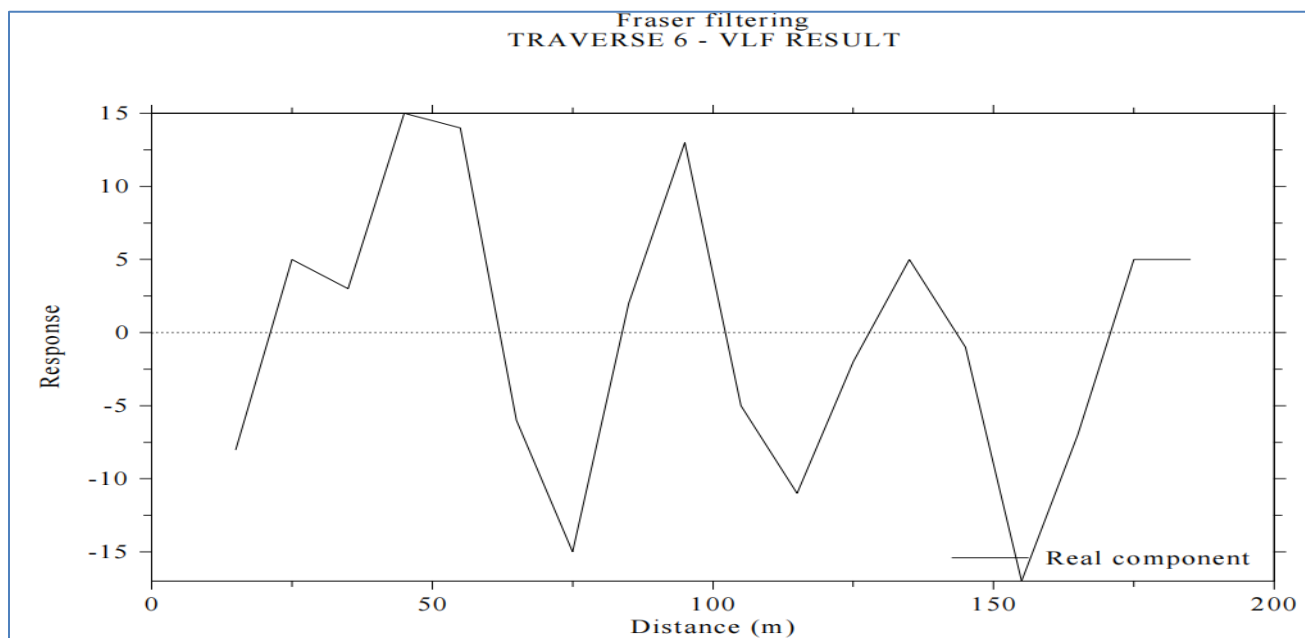


Figure 4.1.6: Fraser Filter Result along Traverse VLF-ORU6

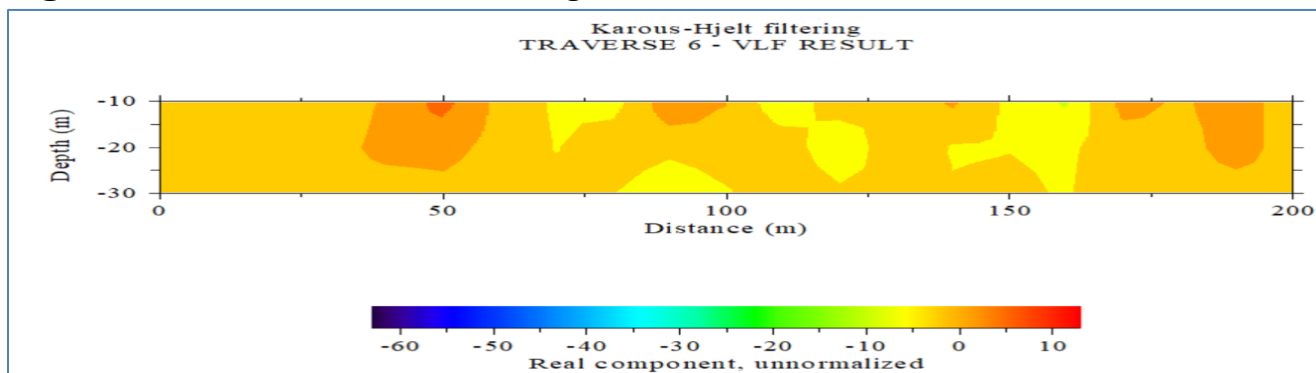


Figure 4.2.6: 2-D Conductivity Section along Traverse VLF-ORU6

4.7 2-D Conductivity Section along Traverse VLF-ORU7

Figures 4.1.7 and 4.2.7 represent the Fraser filtering and 2-D conductivity section results generated for traverse 7. The 2-D section investigated up to 30 m depth beneath the subsurface. The real and imaginary components vary between -22 to -8 and -17 to $+16$. From the 2-D conductivity section, two (2) high conductivity /zones were identified at lateral distances of about 30 m to 45 m and 170 m to 190 m. These zones are suggestive of possible zones for groundwater accumulation.

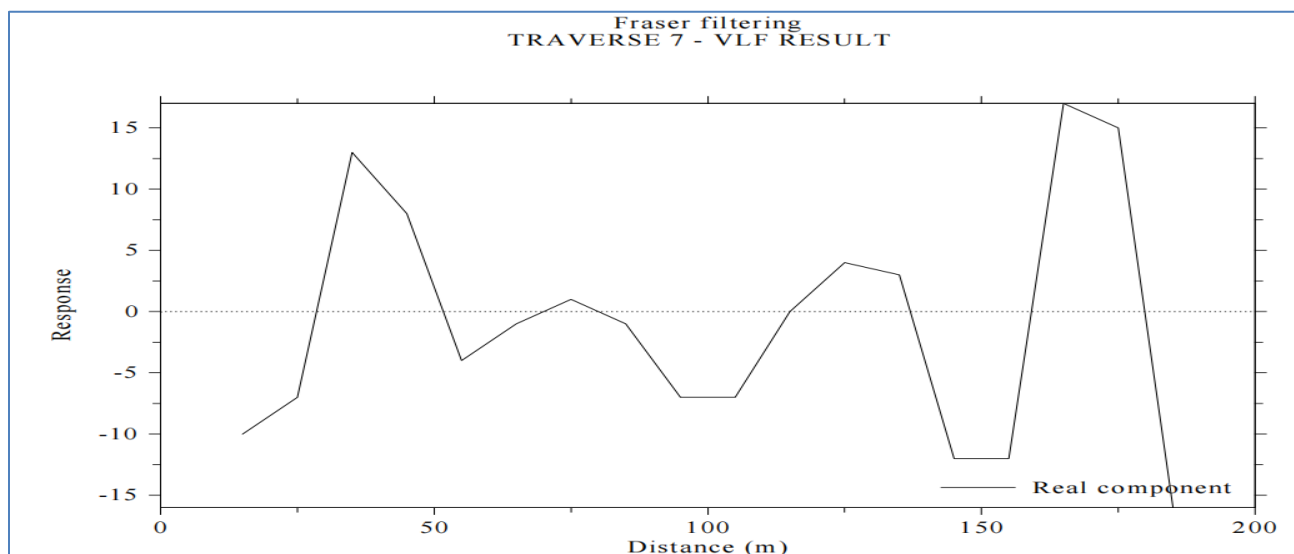


Figure 4.1.7: Fraser Filter Result along Traverse VLF-ORU7

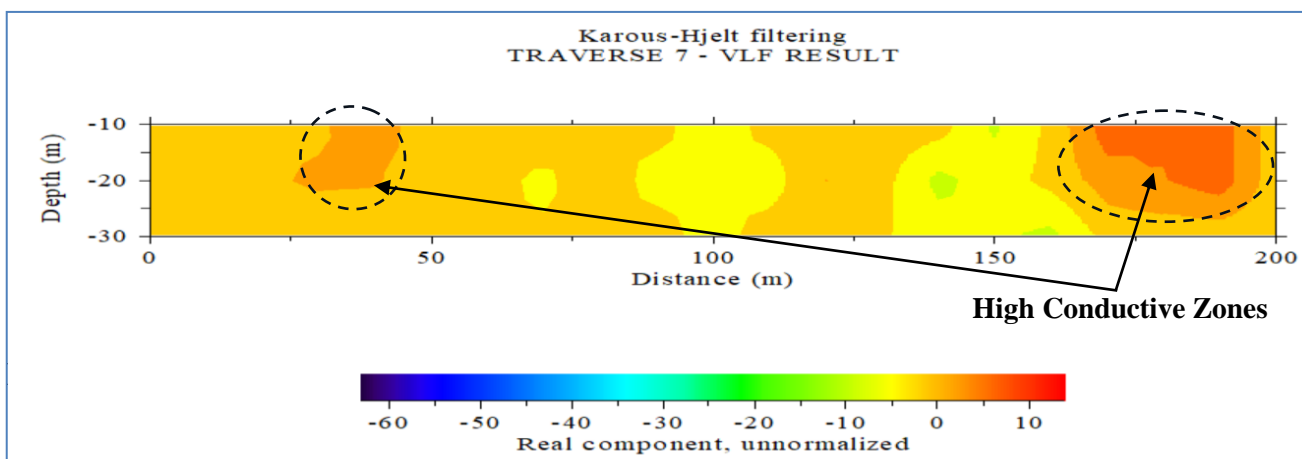


Figure 4.2.7: 2-D Conductivity Section along Traverse VLF-ORU7

Ishola S. A

4.8 2-D Conductivity Section along Traverse VLF-ORU8

Figures 4.1.8 and 4.2.8 represent the Fraser filtering and 2-D conductivity section results generated for traverse 8. The 2-D section investigated up to 30 m depth beneath the subsurface. The real and imaginary components vary between -15 to -2 and -11 to $+14$. From the 2-D conductivity section, there is no major zone of interest (high conductive zone) that could represent a possible fractured zone for groundwater exploration.

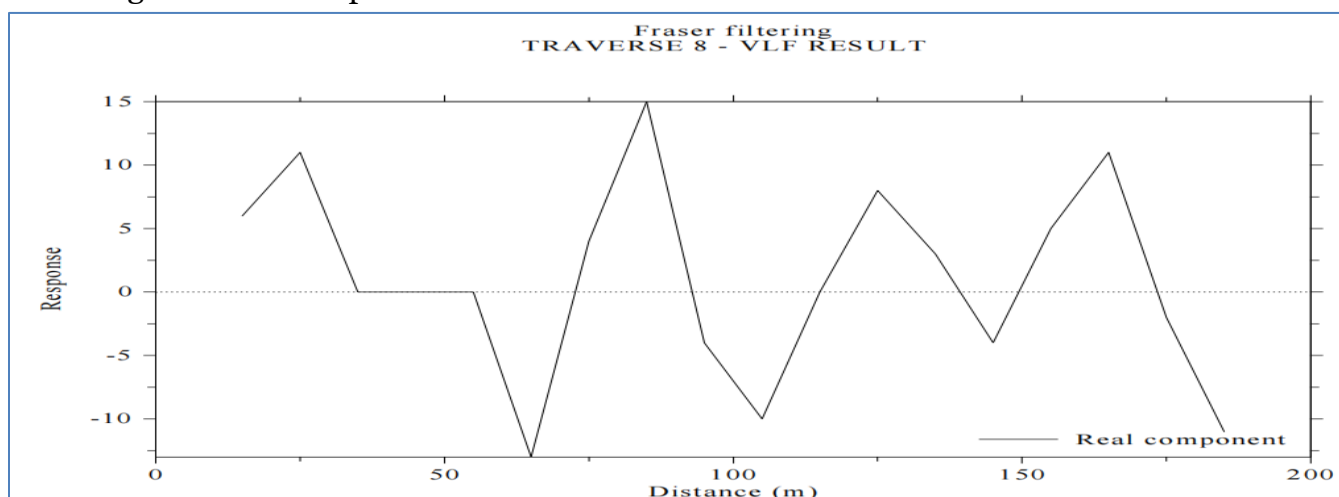


Figure 4.1.8: Fraser Filter Result along Traverse VLF-ORU8

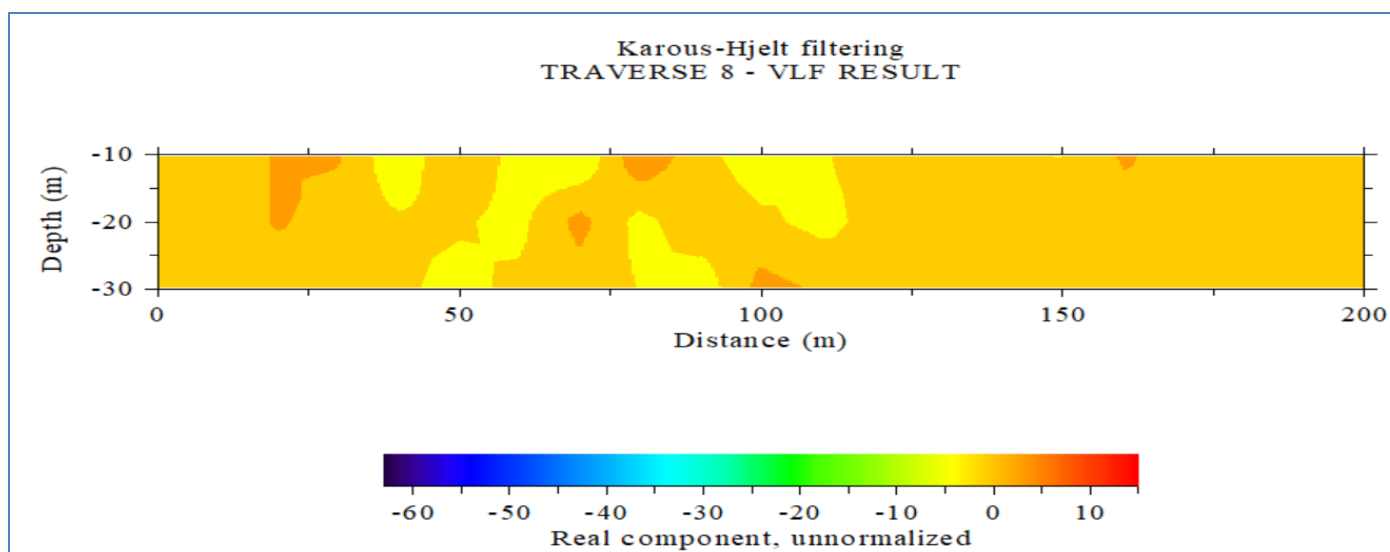


Figure 4.2.8: 2-D Conductivity Section along Traverse VLF-ORU8

Ishola S. A

4.9 2-D Conductivity Section along Traverse VLF-ORU9

Figures 4.17 and 4.18 represent the Fraser filtering and 2-D conductivity section results generated for Traverse 9. The 2-D section investigated up to 30 m depth beneath the subsurface. The real and imaginary components vary between -25 to -3 and $+1$ to $+20$. From the 2-D conductivity section, two (2) high conductivity /zones were identified at lateral distances of about 20 m to 57 m and 80 m to 115 m. These zones are suggestive of possible zones for groundwater accumulation.

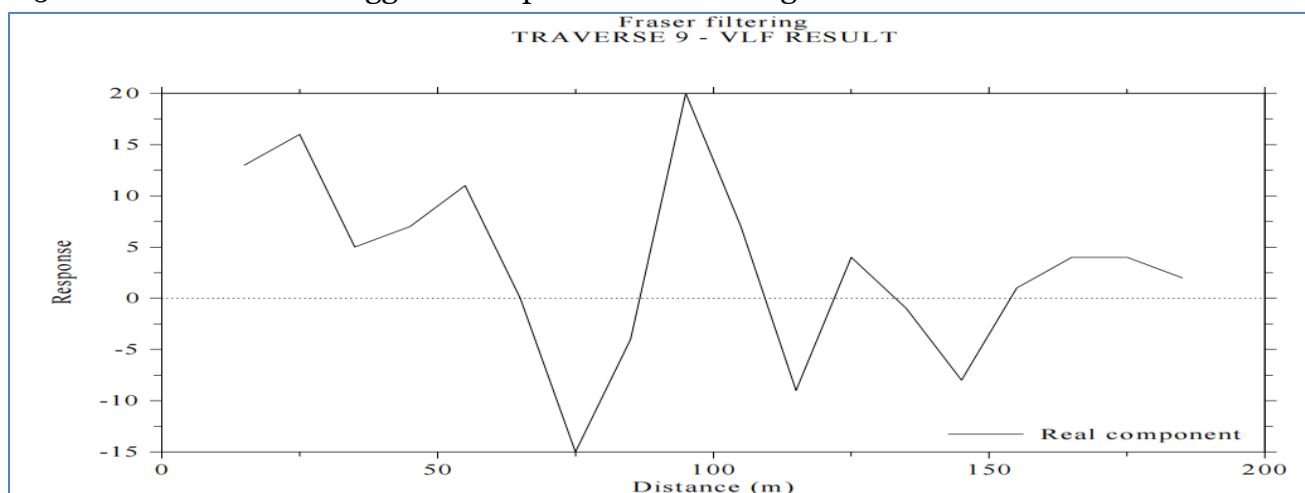


Figure 4.1.0: Fraser Filter Result along Traverse VLF-ORU9

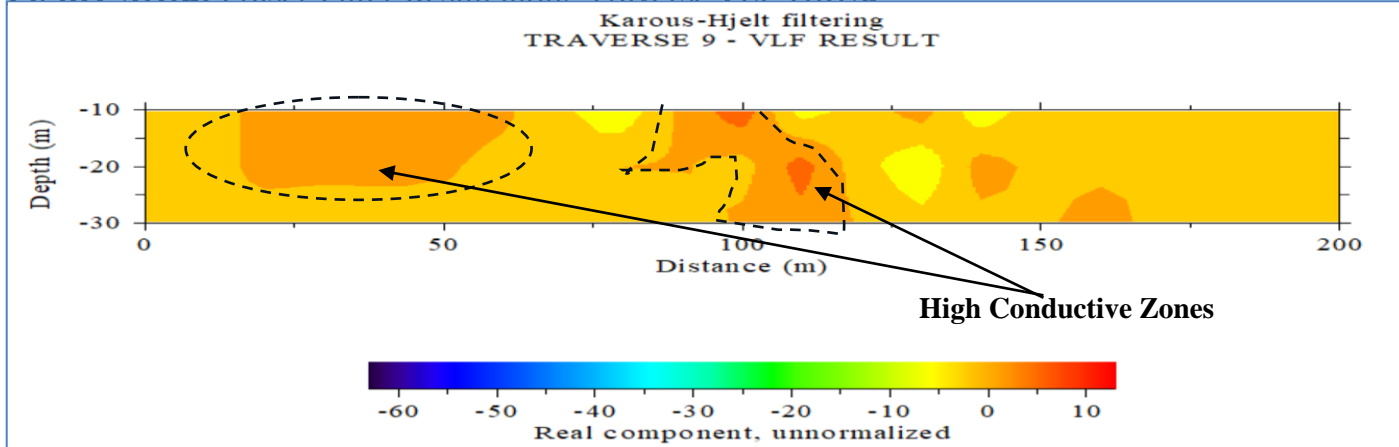


Figure 4.2.9: 2-D Conductivity Section along Traverse VLF-ORU9

4.10 2-D Conductivity Section along Traverse VLF-ORU10

Figures 4.1.10 and 4.2.10 represent the Fraser filtering and 2-D conductivity section results generated for Traverse 10. The 2-D section investigated up to 15 m depth beneath the subsurface. The real and imaginary components vary between -13 to $+7$ and -1 to $+27$. From the 2-D conductivity section, one (1) high conductivity /zone is identified at a lateral distance of about 48 m to 57 m. This zone is suggestive of a possible zone for groundwater accumulation (Figure 4.2.10).

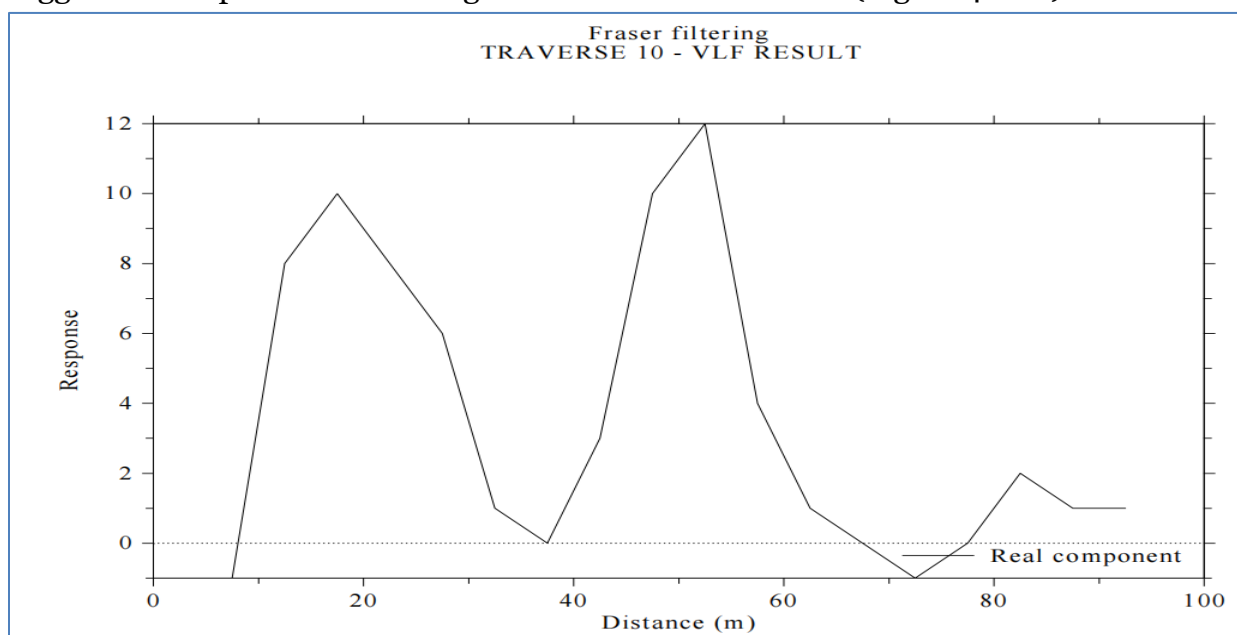


Figure 4.1.10: Fraser Filter Result along Traverse VLF-ORU10

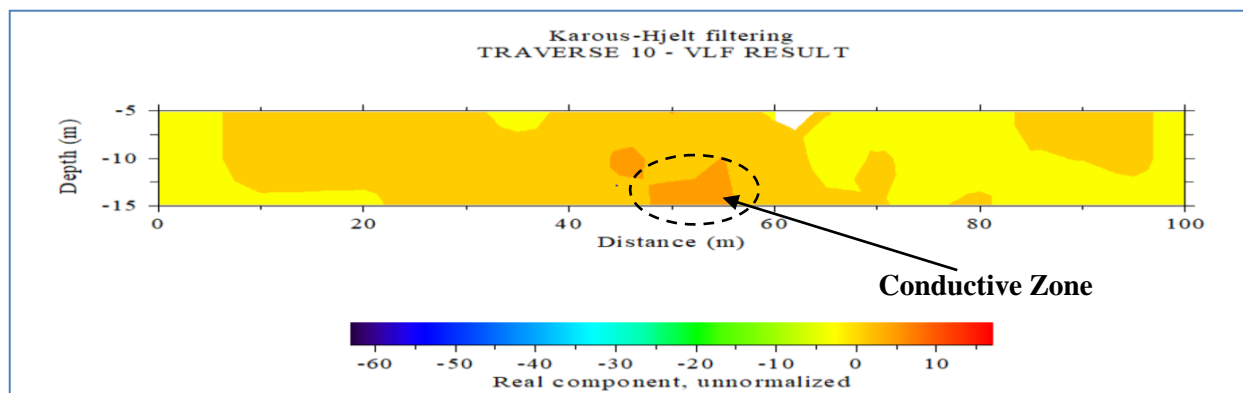


Figure 4.2.10: 2-D Conductivity Section along Traverse VLF-ORU10

Ishola S. A

4.11 2-D Conductivity Section along Traverse VLF-ORU11

Figures 4.1.11 and 4.2.11 represent the Fraser filtering and 2-D conductivity section results generated for Traverse 11. The 2-D section investigated up to 15 m depth beneath the subsurface. The real and imaginary components vary between -10 to $+10$ and $+3$ to $+24$. From the 2-D conductivity section, one (1) high conductivity /zone is identified at a lateral distance of about 46 m to 53 m. This zone is suggestive of a possible zone for groundwater accumulation (Figure 4.2.11).

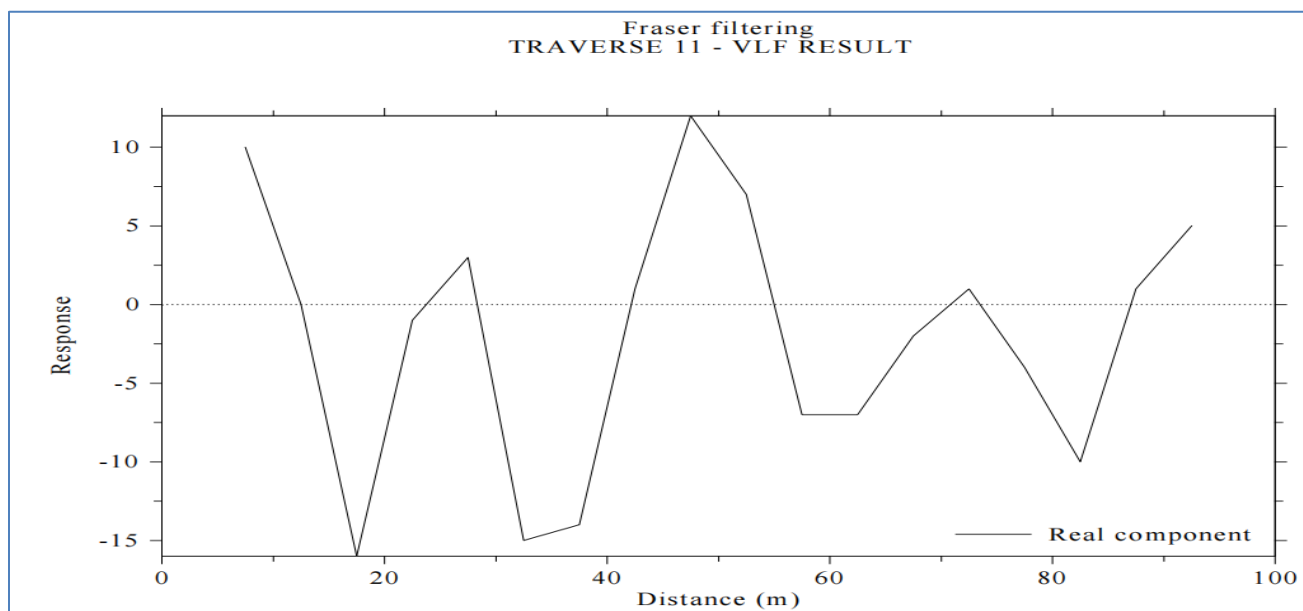


Figure 4.1.11: Fraser Filter Result along Traverse VLF-ORU11

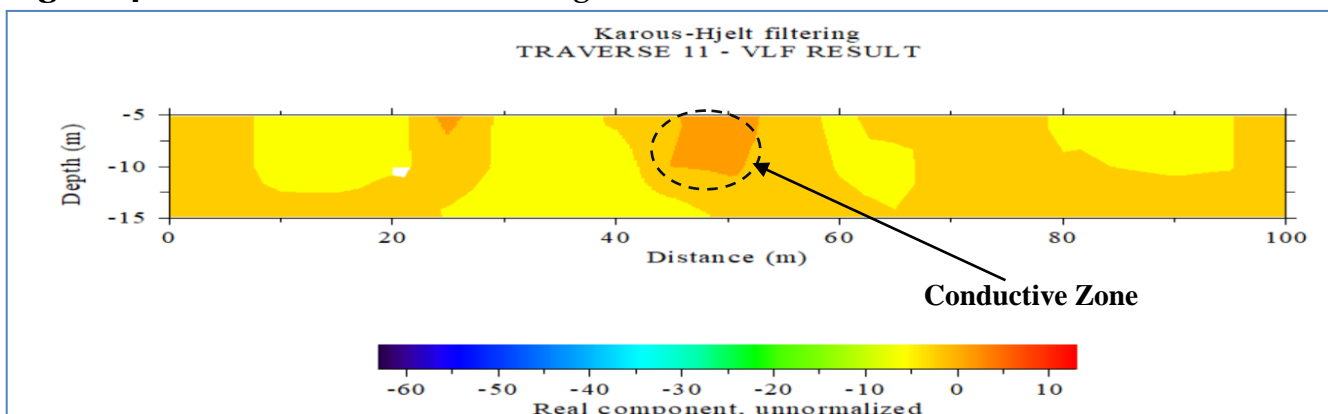


Figure 4.2.11: 2-D Conductivity Section along Traverse VLF-ORU11

4.12 2-D Conductivity Section along Traverse VLF-ORU12

Figures 4.23 and 4.24 represent the Fraser filtering and 2-D conductivity section results generated for Traverse 12. The 2-D section investigated up to 15 m depth beneath the subsurface. The real and imaginary components vary between -24 to -2 and -10 to $+15$. From the 2-D conductivity section, three (3) high conductivity /zones were identified at lateral distances of about 10 m to 15 m, 50 m to 62 m, and 83 m to 100 m. These zones are suggestive of possible zones for groundwater accumulation.

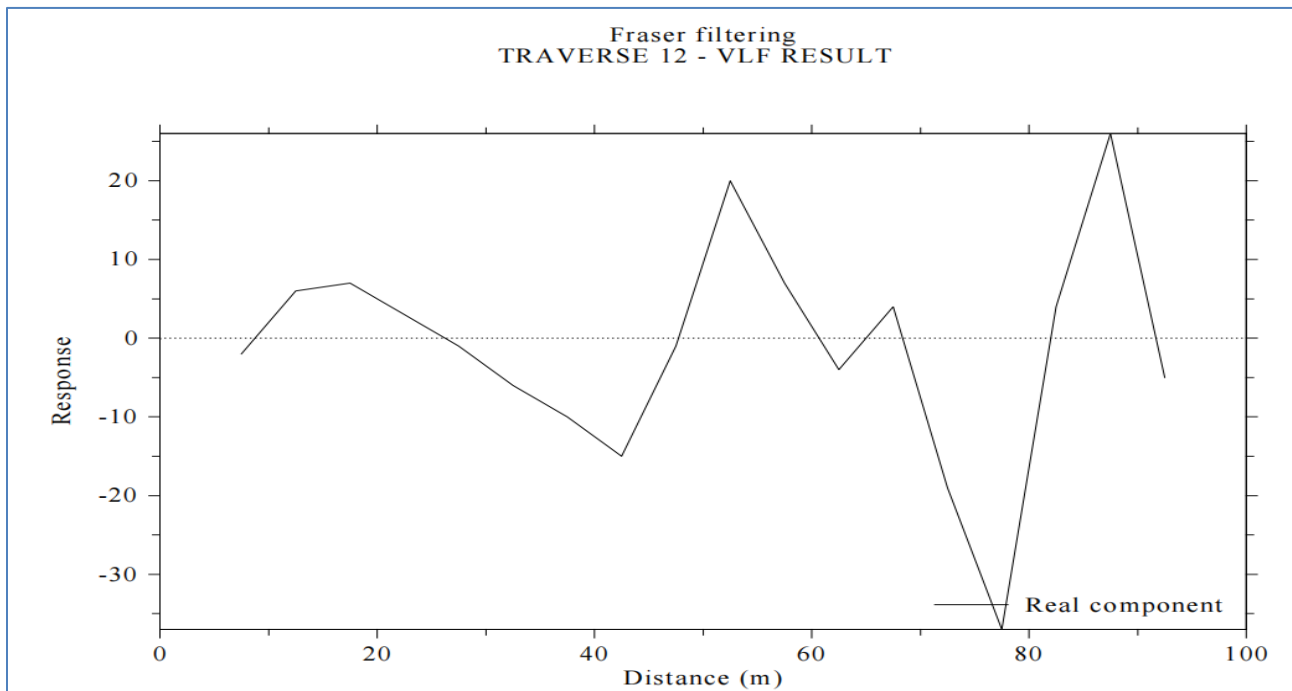


Figure 4.1.12: Fraser Filter Result along Traverse VLF-ORU12

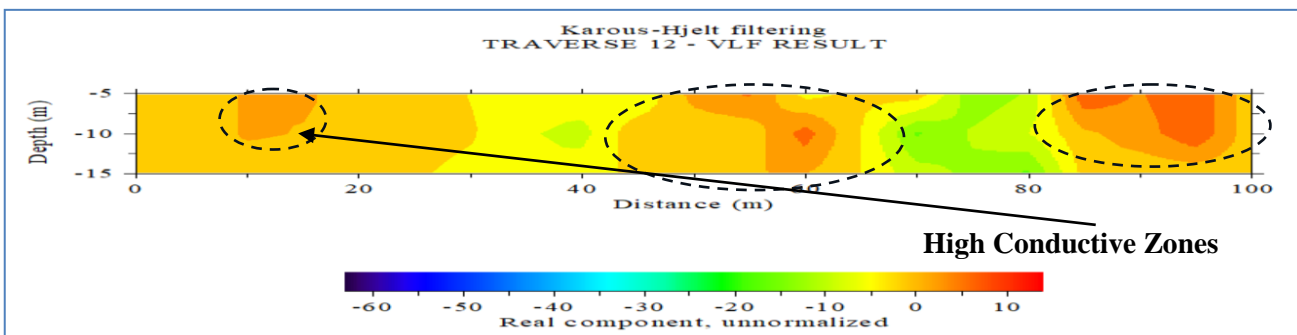


Figure 4.2.12: 2-D Conductivity Section along Traverse VLF-ORU12

Ishola S. A



CONCLUSION: The study area Oru-Ijebu, having been hydro-geologically delineated from the interpretation of VLF data has shown the very low-frequency electromagnetic method is a better, more effective, and economical method to investigate the hydrologic condition and preliminary subsurface investigation of the study area for groundwater exploration and development. The presence of and interconnectivity of fracture zones in the study area showed that the area has good prospects for groundwater development. It is therefore recommended that the search for groundwater in the study area should be aimed at searching for fracture zones where overburden is relatively thin and any borehole drilled in the study area should be made to pass through as many fracture zones as possible. In the study area, VLF-EM survey was carried out along twelve (12) traverses showed high conductive zones indicative of fractured zones with a depth range of 0 to 30m within the subsurface. The conductive zone identified at each traverse are located at 50-75m, 120-165m, 30-50m, 165-200m, 170-190m and 83-100m respectively along the profile. The most conductive zone was found at VLF-ORU03 at a lateral extent of 70-105m, while the least conductive zone was identified at VLF-ORU01 at a lateral extent of 125-165m. The presence and interconnectivity of the fractured zones shows that the study area has good prospects for groundwater development (George et al., 2013). It can thus be concluded that the drilling of productive and

sustainable boreholes suited for groundwater exploration are recommended at various traverses (VLF-ORU01, VLF-ORU02, VLF-ORU03, VLF-ORU04, VLF-ORU05, VLF-ORU07, and VLF-ORU012). These aforementioned locations are prospective sites for further investigation for groundwater development in the study area.

ACKNOWLEDGEMENTS

The author wishes to acknowledge the cooperation of community Heads and the youths of the area in which this research was carried out.

REFERENCES

- Adekoya, S. A., Coker, J. O., & Adenuga, O. O. (2017). Characterization of aquifer using geostatistical analysis of the geoelectrical parameters of Ijebu Igbo, South-West Nigeria. *Journal of Scientific and Engineering Research*, 4(7), 74–81.
- Adesanya, E. (2018). Climate change impact on rainfall and temperature distributions over West Africa from three IPCC scenarios. 2018 IPCC Report.
- Alagbe, O. A., Sunmonu, L. A., & Adabanija, M. A. (2013). *Research Journal of Physical Sciences*, 1(3), 1–5.
- Anbazhagan, S., Balamurugan, G., & Biswal, T. K. (2011). Remote sensing in delineating deep fracture aquifer zones. In S. Anbazhagan, S. K. Subramanian, & X.



- Yang (Eds.), *Geoinformatics in Applied Geomorphology* (pp. 205–229). CRC Press, Taylor and Francis.
- Ariyo, S. O., & Osinowo, O. O. (2007). Hydrogeophysical investigation for groundwater at Atan/Odosenbora area, southwest Nigeria. *Ife Journal of Science*, 9, 87–92.
- Auken, E., & Christiansen, A. V. (2004). Layered and laterally constrained 2D inversion of resistivity data. *Geophysics*, 69(3), 752–761.
- Awosika, D. D., Ariyibi, E. A., Adebayo, A. S., Dasho, O. A., Shode, O. H., Adenika, C. I., & Olagunju, E. (2020). Evaluation of groundwater potential zones using integrated geophysical approach in Obun-Ewi, Ondo East Local Government, Southwestern Nigeria. *Sustainable Water Resources Management*, 6, 1–12.
- Bayewu, O. O., Oluruntola, M. O., & Mosuro, G. O. (2017). Geophysical evaluation of groundwater potential in part of southwestern basement complex terrain, Nigeria. *Applied Water Science*, 7, 4615–4620. <https://doi.org/10.1007/s13201-017-0623-4>
- Bayewu, O. O., Oloruntola, M. O., Mosuro, G. O., & Watabuni, F. G. (2012). Groundwater exploration in Ago-Iwoye area of southwestern Nigeria using Very Low Frequency Electromagnetic (VLF-EM) and electrical resistivity methods. *International Journal of Applied Sciences and Engineering Research*, 1(3), 452–462. <https://doi.org/10.6088/ijaser.0020101046>
- Chave, A. D., & Jones, A. G. (2012). *The Magnetotelluric Method: Theory and Practice*. Cambridge University Press.
- Everett, M. E. (2013). *Near-Surface Applied Geophysics*. Cambridge University Press.
- George, A. M., Okwueze, E. E., Akpan, A. E., & Uchegbu, C. J. (2008). *Nigerian Journal of Physics*, 20(1), 136–144.
- George, A. M., Abong, A. A., & Obi, D. A. (2013). Fracture zone detection using very low frequency (VLF) electromagnetic method in parts of Oban Massif, southeastern Nigeria. *Advances in Applied Science Research* (Pelagia Research Library).
- Haeni, F. P., Lane, J. W., & Lieblich, D. A. (1993). *Memories of the XXIVth Congress, Oslo, Norway: International Association of Hydrogeologists*, 577–587.
- Hecht, E. (2002). *Optics* (4th ed.). Addison-Wesley.



- Ishola, S. A. (2024). Groundwater protection assessment using frequency domain electromagnetic method and direct current electrical resistivity method in Papalanto, South-West Nigeria. *Nigerian Journal of Theoretical and Environmental Physics*, 2(1), 1–27. <https://doi.org/10.62292/njtep.v2i1.2024.1>
- Ishola, S. A., & Olufemi, S. T. (2024). Groundwater exploration using geoelectric technique in Oru-Ijebu, South-West Nigeria. *Nigerian Journal of Theoretical and Environmental Physics*, 2(1), 49–66.
- Jamal, N., & Singh, N. P. (2018). Identification of fracture zones for groundwater exploration using VLF-EM and ER methods in the hard rock area of Sandog Block, India. *Science Direct*, 7, 195–203.
- Jansein, J., & Jurcek, P. (1993). *Environmental and Engineering Geophysical Society*, Volume II, 635–644.
- Jegade, S. I., Osazuwa, I. B., Ujuanbi, O., & Chiemekwe, C. C. (2011). *International Journal of Physical Sciences*, 2(6), 1–8.
- Lieblich, D. A., Lane, J. W., & Haeni, F. P. (1991). In *Expanded Abstracts with Bibliographies*, SEG Annual International Meeting, vol. 1, p. 23.
- Mansour, K., Omar, K., Ali, K., & Zaher, M. A. (2018). Geophysical characterization of the role of fault and fracture systems for recharging groundwater aquifers from surface water of Lake.
- McNeill, J. D. (1980). *Electromagnetic terrain conductivity measurement at low induction numbers*. Geonics Limited Technical Note TN-6.
- McNeill, J. D., & Labson, V. F. (1991). In M. C. Nabighian (Ed.), *Society of Exploration Geophysicists*, 191–218.
- Mushtaq, F., Zahid, M., Bhatti, I. A., Nasir, S., & Hussain, T. (2019). Possible applications of coal fly ash in wastewater treatment. *Journal of Environmental Management*, 240, 27–46.
- Milsom, J., & Eriksen, A. (2011). *Field Geophysics*. Wiley-Blackwell.
- Nabighian, M. N. (1988). *Electromagnetic Methods in Applied Geophysics*. SEG Books.
- Okafor, P., & Mamah, L. (2012). Integration of geophysical techniques for groundwater potential investigation in Katsina-Ala, Benue State, Nigeria. *Pacific Journal of Science and Technology*, 13(2), 463–474.
- Oketayo, A. N., Opaleye, D. O., Ademola, J. A., Alpha, P. N., & T. A. (2022). Perception



of rice farmers on climate variability in Oru-Ijebu, Ogun State. *Quest Journals Journal of Research in Environmental and Earth Sciences*, 8(8), 34–40.

Holocene tufa system in the Lathkill Valley, N. Derbyshire using ground-penetrating radar. *Sedimentology*, 47, 721–737.

Oketayo, O. O., Akinnubi, R. T., Adeyemi, F. O., Ayanda, O. S., & Nelana, S. N. (2022). Assessment of drinking water samples around selected oil spillage and metal recycling company in Lagos State, Nigeria: Heavy-metals in drinking waters. *African Scientific Reports*, 1(3), 154–160.

Reynolds, J. M. (1997). *An Introduction to Applied and Environmental Geophysics*. Wiley.

Reynolds, J. M. (2011). *An Introduction to Applied and Environmental Geophysics* (2nd ed.). Wiley.

Osinowo, O. O., & Olayinka, A. I. (2012). VLF-EM and ER investigation for groundwater potential evaluation in a complex geological terrain around the Ijebu-Ode transition zone, southwestern Nigeria. *Journal of Geophysics and Engineering*, 372–396. <https://doi.org/10.1088/1742-2132/9/4/374>

Salvam, S., Magesh, N. S., Chidambaram, S., & Rajamanickam, M. (2015). A GIS-based identification of groundwater recharge potential zones using RS and IF technique: A case study in Ottapidaram Taluk. *Environmental Earth Science*, 73(7), 3785–3788.

Sharma, S. P., & Baranwal, V. C. (2005). *Journal of Earth System Science*, 114, 515–528.

Ozegin, K. O., & Oseghale, A. O. (2012). Geophysical characterization of shallow aquifers in a sedimentary area: A case study. *Advances in Applied Science Research*, 3(1), 469–474.

Smith, K. H., & Johnson, L. M. (2007). Groundwater quality assessment using VLF-EM and electrical resistivity methods in a granitic basement terrain: A case study of Iyekeogba. *Geophysics International*, 42, 185–201.

Parasnis, D. S. (1996). *Principles of Applied Geophysics* (5th ed.). Chapman and Hall.

Peedley, H. M., Hill, I., & Brassington, J. (2000). Three-dimensional modeling of a